CENTER FOR DRUG EVALUATION AND RESEARCH

APPLICATION NUMBER:

125547Orig1s000

PHARMACOLOGY REVIEW(S)

MEMORANDUM

Portrazza (necitumumab)

Date: September 10, 2015
To: File for BLA 125547
From: John K. Leighton, PhD, DABT
Director, Division of Hematology Oncology Toxicology
Office of Hematology and Oncology Products

I have examined pharmacology/toxicology review for Portrazza conducted by Drs. Brower and Weis, and secondary memorandum and labeling provided by Dr. Helms. No exposure margins are included in the pregnancy risk statement (section 8.1 of the label) as no embryo-fetal developmental toxicology studies were conducted with necitumumab and the mouse studies were conducted in knockout models, not animals treated with an anti-EGFR antibody.

I concur with Dr. Helms' conclusion that Portrazza may be approved for the proposed indication.

This is a representation of an electronic record that was signed electronically and this page is the manifestation of the electronic signature.

/s/

JOHN K LEIGHTON
09/10/2015

MEMORANDUM

Date: July 24, 2015
From: Whitney S. Helms, PhD
Pharmacology Supervisor
Division of Hematology Oncology Toxicology for Division of Oncology Products 2
To: File for BLA # 125547
PORTRAZZA (necitumumab)
Re: Approvability of Pharmacology and Toxicology

On, December 2, 2014 Eli Lilly submitted biological license application (BLA) 125547 for necitumumab in combination with gemcitabine and cisplatin for the first line treatment of patients with locally advanced or metastatic squamous non-small cell lung cancer (NSCLC). Non-clinical studies examining the pharmacology and toxicology of necitumumab provided to support BLA 125547 were reviewed in detail by Margaret E. Brower, PhD and Shawna L. Weis, PhD. The findings of these studies are summarized in the "Executive Summary" of the BLA review and reflected in the product label.

Necitumumab is a fully human IgG1 monoclonal antibody targeting the epidermal growth factor receptor (EGFR). Necitumumab binds to domain III of EGFR, one of the external domains involved in ligand binding. Binding of necitumumab to EGFR prevents ligand binding to the receptor, resulting in inhibition of downstream signaling from the receptor. Binding of the antibody also leads to receptor internalization, further limiting EGFR signaling in targeted cells. In addition, necitumumab has potential Fc function and was able to mediate antibody dependent cellular cytotoxicity in in vitro assays. Consistent with other approved antibodies that target EGFR, the established pharmacological class for necitumumab is epidermal growth factor receptor antagonist.

Necitumumab bound to EGFR from humans and cynomolgus monkeys with similar affinity, thus, general toxicology studies were conducted in cynomolgus monkeys. Monkeys were administered necitumumab weekly for 5 or 26 weeks to investigate the safety of the antibody. In the 26 week study the skin and injection site were the primary targets for necitumumab-mediated toxicity. Findings included dose-dependent increases in hyperkeratosis, hyperplasia, hemorrhage, inflammation and lymphocytic infiltration at all doses tested. Skin toxicities were the most commonly observed adverse events clinically as well. In monkeys mild but persistent decreases in magnesium levels did occur following administration of necitumumab. More significant and potentially fatal hypomagnesemia occurred clinically. Thromboembolism observed in the clinic was not exhibited in monkeys, though mild increases in platelets and fibrinogen occurred at all dose levels compared to controls throughout the 26-week study and extending until the end of the 8 week recovery period.

Consistent with the ICH S6 guidance, genetic toxicology studies were not conducted or required for necitumumab. Carcinogenicity studies were not required to support the licensing application for a product to treat advanced human cancer and are neither planned nor expected as post-marketing requirements at this time.

No dedicated studies examining the potential for reproductive toxicity were conducted using necitumumab. Instead, Eli Lilly submitted a literature based assessment of the potential effects of the blocking EGFR signaling on a developing embryo. Based on the presented literature, disruption of EGFR can have clear detrimental effects, including significant effects on placental, lung, skin, cardiac, and neural development which can lead to embryofetal and postnatal death, as well as clear phenotypic signs of teratogenicity. This assessment was primarily derived from observations in total or partial EGFR knockout animals. In order look specifically at potential developmental effects following an anti-EGFR antibody, the Applicant provided data by right of reference to a developmental study in non-human primates conducted using cetuximab. Cetuximab binds to a similar epitope and has comparable in vitro and in vivo pharmacologic effects as necitumumab. The pharmacological and pharmacokinetic data comparing necitumumab and cetuximab are reasonable to support the use of cetuximab as a surrogate for the purpose of investigating the potential for necitumumab to have effects on a developing organism. Administration of cetuximab during development resulted in embryolethality and abortions at clinically relevant doses of the antibody. The totality of the data suggests that necitumumab has the potential to cause serious adverse effects in a developing fetus. Necitumumab is, therefore, not recommended for use during pregnancy. Based on a half-life of approximately 12 days, use of contraception for 3 months following the final dose of the antibody is recommended for females of reproductive potential.

Recommendations: I concur with the conclusions of Drs. Brower and Weis that the pharmacology and toxicology data are sufficient to support the approval of BLA 125547 for Portrazza in combination with gemcitabine and cisplatin for the treatment of patients with squamous cell NSCLC. There are no outstanding nonclinical issues that would prevent the approval of Portrazza for the treatment of the intended patient population.

This is a representation of an electronic record that was signed electronically and this page is the manifestation of the electronic signature.

/s/

WHITNEY S HELMS
07/24/2015

DEPARTMENT OF HEALTH AND HUMAN SERVICES
PUBLIC HEALTH SERVICE
FOOD AND DRUG ADMINISTRATION
CENTER FOR DRUG EVALUATION AND RESEARCH

PHARMACOLOGY/TOXICOLOGY BLA REVIEW AND EVALUATION

Application number:	BLA 125547
Supporting document/s:	0002
Applicant's letter date:	December 2, 2014
CDER stamp date:	December 2, 2014
Product:	Necitumumab (Portrazza)
Indication:	Locally advanced or Metastatic Squamous Non-Small Cell Lung Cancer (NSCLC) in combination with gemcitabine-cisplatin
Applicant:	Eli Lilly and Co.
Review Division:	Division of Hematology Oncology Toxicology (Division of Oncology Products 2)
Reviewer:	Margaret E. Brower, PhD, Shawna L. Weis, PhD
Supervisor/Team Leader:	Whitney S. Helms, PhD
Division Director:	John K. Leighton, PhD (Patricia Keegan, MD)
Project Manager:	Mimi Biable, MS

Disclaimer

Except as specifically identified, all data and information discussed below and necessary for approval of BLA 125547 are owned by Eli Lilly or are data for which Eli Lilly has obtained a written right of reference. Any information or data necessary for approval of BLA 125547 that Eli Lily does not own or have a written right to reference constitutes one of the following: (1) published literature, or (2) a prior FDA finding of safety or effectiveness for a listed drug, as reflected in the drug's approved labeling. Any data or information described or referenced below from reviews or publicly available summaries of a previously approved application is for descriptive purposes only and is not relied upon for approval of BLA 125547.

TABLE OF CONTENTS

Table of Tables

Table of Figures

1 Executive Summary

1.1 Introduction

Eli Lilly has submitted Biologics License Application (BLA) 125547 for necitumumab in combination with gemcitabine and cisplatin for the first-line treatment of patients with locally advanced or metastatic squamous non-small cell lung cancer (NSCLC). The recommended clinical dose of necitumumab is 800 mg administered as an intravenous infusion once daily on Days 1 and 8 of each 3-week cycle. Nonclinical pharmacology, pharmacokinetic, and toxicology studies have been submitted to support the approval of necitumumab for the proposed indication.

1.2 Brief Discussion of Nonclinical Findings

Necitumumab is a human IgG_1 monoclonal antibody that binds to the extracellular domain of the human epidermal growth factor receptor (EGFR) and blocks interaction between EGFR and its ligands, resulting in inhibition of activation of EGFR and downstream signaling from the receptor. Besides inhibition of receptor dimerization and ligand binding, the antibody is able to mediate antibody dependent cell cytotoxicity, potentially contributing to its overall activity against EGFR-expressing cells. Treatment of mice implanted with tumor cell lines derived from NSCLC, pancreatic, and colorectal tumors with necitumumab resulted in varying degrees of tumor growth inhibition, depending, in part, on EGFR status of cells. The addition of necitumumab also improved the anti-tumor activity of the combination of cisplatin and gemcitabine compared to either the antibody alone or the gemcitabine/cisplatin only combination in some in vivo tumor implant models. Necitumumab binds specifically to EGFR and not to other members of the EGFR family and has similar affinities for the human and cynomolgus monkey proteins. This similarity in binding along with generally similar patterns of staining between human and cynomolgus monkey tissues with necitumumab support the use of the monkey as a relevant model for toxicological examination.

Necitumumab was evaluated in 5- and 26-week repeat dose studies in cynomolgus monkeys. There were no significant drug-related findings following dosing for 5 weeks at doses as high as 40 mg/kg. In the 26-week study, monkeys were treated at dose levels of 0, 6, 19, or 60 mg/kg weekly for 26 weeks. Following 26 weeks of dosing, the skin was found to be the primary target site. Hyperplastic dermatitis, characterized by epidermal hyperplasia, hyperkeratosis, and inflammatory infiltration was observed grossly and microscopically in skin of the abdomen, inguinal area, ears /nose/mouth, and to a lesser extent, skin of the mammary glands. These findings were observed at all dose levels with a higher incidence at 19 and 60 mg/kg. Skin at the injection site exhibited hyperkeratosis, hyperplasia, hemorrhage, inflammation, and lymphocytic infiltration at all doses with a greater incidence at the 60 mg/kg dose level. Clinical observations were consistent with dose-related skin toxicity and included erythema, scaling, dry skin, and rash. Skin toxicity has previously been observed with similar EGFR inhibitors (e.g. cetuximab) and is a major adverse reaction clinically. Magnesium levels were marginally depressed in males and depressed in females at doses ≥ 19 mg/kg. This finding is consistent with hypomagnesemia observed in the clinic.

Magnesium levels in monkeys remained marginally depressed at the end of the recovery period.

Degeneration of renal tubular epithelium was observed in monkeys administered necitumumab; this finding was consistent with findings observed with cetuximab. Diffuse inflammation and lymphocytic infiltration was observed in multiple organs and tissues following dosing and recovery at all dose groups. Thromboembolism observed in the clinic did not occur in monkeys, though mild increases in platelets and fibrinogen occurred at all dose levels compared to controls throughout the 26-week study and extending until the end of the recovery period, suggesting the potential for effects on coagulation. Toxicokinetic data in this study indicated that necitumumab exposure was generally dose proportional to greater than dose-proportional in monkeys treated for 26 weeks; the 19 mg/kg dose appeared to be similar to the C_{max} and AUC of 629 µg/mL and 105000 µg·h/mL, respectively, observed in humans at the recommended dose of 800 mg. Necitumumab exhibited a long terminal half-life in monkeys (~145 h) which was less than that observed in humans (~286 hours).

Reproductive toxicity studies with necitumumab were not conducted. Instead, the Applicant submitted a literature-based assessment of the antibody's potential for reproductive toxicity. Based on these data, disruption or depletion of EGFR is associated with significant developmental consequences including effects on placental, lung, cardiac, skin, and neural development. In mice, the absence of EGFR signaling resulted in embryolethality as well as post-natal death in multiple genetic backgrounds. In addition to the data from the literature demonstrating the importance of EGFR to development, the Applicant presented findings from the reproductive toxicology for cetuximab, reviewed under BLA 125084, for which the Applicant has the right of reference. To support its relevance as a developmental surrogate for necitumumab, the Applicant demonstrated that cetuximab and necitumumab bind to a similar epitope in the EGFR III domain and that in both in vivo and in vitro studies the antibodies had comparable activity. Cetuximab was detected in amniotic fluid and the serum of embryos from treated dams and caused embryolethality and abortions at doses of 1.6 to 4 times the recommended human dose. Necitumumab has the potential to cause fetal harm when administered to pregnant women based on the cetuximab data and the data showing that EGFR signaling is essential for normal organogenesis, proliferation, and differentiation in the developing embryo. A warning for embryofetal risk is warranted in the label.

1.3 Recommendations

1.3.1 Approvability

From the nonclinical perspective, necitumumab is approvable in combination with gemcitabine and cisplatin for the first-line treatment of patients with locally advanced or metastatic squamous non-small cell lung cancer (NSCLC).

1.3.2 Additional Non Clinical Recommendations

None

1.3.3 Labeling

A separate labeling review will be completed, as necessary.

2 Drug Information

2.1 Drug

CAS Registry Number
906805-06-9

Generic Name
Necitumumab

Code Name
IMC-11F8; LY3012211

Chemical Name
Immunoglobulin G1, anti-(human endothelial growth factor receptor (receptor tyrosine protein kinase ErbB1, EC 2.7.10.1)); human monoclonal IMC-11F8 γ1 heavy chain (224-214')-disulfide with human monoclonal IMC-11F8 κ light chain dimer (230-230":233-233")-bisdisulfide

Molecular Formula/Molecular Weight
Molecular formula not provided/ Molecular weight = (b) (4) kDa

Figure 1: Structure of Necitumumab

Pharmacologic Class
Epidermal growth factor receptor (EGFR) anatagonist

2.2 Relevant INDs

IND 102,512

2.3 Drug Formulation

Table 1: Necitumumab drug product formulation (800 mg/50 mL)

Ingredient	Quantity (mg/mL)	Function	Reference to Standards
Active Ingredient			
Necitumumab	16	Active Ingredient	In-house
Other Ingredients			
Sodium Citrate, Dihydrate	2.55	(b) (4)	USP-NF, Ph. Eur., JP
Citric Acid, Anhydrous	0.256		USP, Ph. Eur., JP
Glycine	9.984		USP, Ph. Eur., JP
Sodium Chloride	2.338		USP, Ph. Eur., JP
Mannitol	9.109		USP-NF, Ph. Eur., JP
Polysorbate 80	0.1		USP-NF, Ph. Eur., JP
Water for Injection	*q.s.* (b) (4)		USP, Ph. Eur., JP

q.s. = quantity sufficient

2.4 Comments on Novel Excipients

None

2.5 Comments on Impurities/Degradants of Concern

None

2.6 Proposed Clinical Population and Dosing Regimen

- Indication: First-line treatment of patients with locally advanced or metastatic squamous non-small cell lung cancer (NSCLC).
- Dosing Regimen: 800 mg administered as an intravenous infusion once daily on Days 1 and 8 of each 3-week cycle in combination with gemcitabine and cisplatin

2.7 Regulatory Background

November 2008	IND 102512
October 2013	Fast track designation granted
June 2014	Pre-BLA meeting
December 2014	Rolling BLA submission

3 Studies Submitted

3.1 Studies Reviewed

Pharmacology

- Necitumumab (IMC-11 FS) cross-reactivity with human ErbB2, ErbB3 and ErbB4 receptors (Report 08-13-2013)
- Efficacy of human anti-EGFR mAb C11F7 on A431b epidermoid carcinoma xenografts (Report 1221-02)

- Efficacy of anti-IGF-IR mAb A12, comparison of "corn" (INC-001) and human (INC-11F8) anti-EGFR mAbs to cetuximab in BxPC-3 human pancreatic carcinoma xenografts (Report 1300-02)
- Necitumumab mediated internalization and degradation of EGFR-eGFP (Report 2013-08-15)
- Species cross-reactivity of monoclonal anti-EGFR antibodies (Cetuximab, Necitumumab, Panitumumab and ME-1) (Report 2013-9-10)
- Inhibition of ligand-induced EGFR phosphorylation by necitumumab in LK-2 human squamous lung cancer cells stably overexpressing wild-type human EGFR (Report 2014-03-05)
- Investigation of Ramucirumab ADCC Activity (Report SDR- 13049-00)
- PK/PD Study for IMC-11F8 against BxPC-3 xenografts (Report 2201-03A)
- Effect of necitumumab, a fully human monoclonal antibody against the human epidermal growth factor receptor, on viability of DiFi and NCI-H508 human colon carcinoma cells (Report 2014-03-06)
- Comparison of human anti-EGFR mAb IMC-11F8 and cetuximab on GEO xenografts (Report 3708-06)
- Efficacy study with monoclonal antibody IMC-11F8 (anti-EGFR) in a subcutaneous human NCI-H1975 non-small cell lung cancer (NSCLC) xenograft model (Report 3732-06)
- Efficacy study with monoclonal antibody IMC-11F8 (anti-EGFR) in a subcutaneous human NCI-H292 non-small cell lung cancer (NSCLC) xenograft model (Report 3733-06)
- PK/PD of IMC-11 FS, Cetuximab and Panitumumab in a HCC827 human NSCLC xenograft model (Report 4983-10)
- Efficacy of IMC-11F8 (necitumumab) in NCI-H441 NSCLC xenografts stably overexpressing wild type EGFR (IV-2130) (Report 5227-11)
- NCI-H441 #3HL: Efficacy of Necitumumab (IMC-11 FS) in NCI-H441 NSCLC xenografts stably over-expressing mutated (Δ746-750) EGFR (IV-2132) (Report 5229-11)
- Efficacy of IMC-11 F8 (necitumumab) in a SC xenograft model of NCI-H441 human NSCLC (IV-2152) (Report 5249-11)
- Generation and preclinical characterization of the fully human anti-EGFR monoclonal antibody (IMC-11F8) (Report IMC11F8-01)
- To determine mechanism of action of IMC-11 F8 in combination with gemcitabine + Cisplatin in NCIH1650 NSCLC xenograft model (IV-1600) (Report 4697-10)
- Mechanism of action of IMC-11F8 in combination with gemcitabine and cisplatin in an NCI-H1650 NSCLC xenograft model (IV-1329) (report 4428-09)

Pharmacokinetics

- Study 7573-110: A multiple dose pharmacokinetic study of IMC-11F8 administered to cynomolgus monkeys

General Toxicology/Toxicokinetics

- Study CR0878: 5-week repeat-dose study in monkeys with a 6-week recovery phase

- Study (b) (4) 023.07: A 26-week toxicity, toxicokinetic, and immunogenicity study of IMC-11F8 administered intravenously weekly to cynomolgus monkeys with an 8-week recovery period

- Study (b) (4) 023.07 Final report amendment 1: A 26-week toxicity, toxicokinetic, and immunogenicity study of IMC-11F8 administered intravenously weekly to cynomolgus monkeys with an 8-week recovery period

Cross Reactivity studies

- Study #0409: IHC staining of IMC-11F8 for frozen sections of human, monkey and rat tissues

3.2 Studies Not Reviewed

Secondary Pharmacology

- Effects of IMC-11F8 and CPT-11 on DLD-1 human colon carcinoma xenografts (Report 2075-03)
- Effects of IMC-11F8 and CPT-11 on H-29 xenografts (Report 2076-03)
- A12, IMC-11F8 combination versus a didiabody (noncovalently associated) in a BxPC-3 xenograft model (Report 2148-03)
- Efficacy Study with Monoclonal Antibody IMC-11 F8 (anti-EGFR) in a Subcutaneous Human HCC827 Non-Small Cell Lung Carcinoma (NSCLC) Xenograft Model (Report 3731-06)
- A12-11F8 and IMC-A12 +/-IMC-11F8 Efficacy in a Mia-PaCa-2LP Orthotopic Pancreatic Cancer Model (Report 4498-09)
- Mechanism of action of IMC-11 F8 in combination with Gemcitabine + Cisplatin in an A549 NSCLC xenograft model (IV-160 1) (Report 4698-10)
- Efficacy of IMC-11 F8 in combination with Gemcitabine+Cisplatin, Paclitaxei+Cisplatin or Pemetrexed+Cisplatin in a Calu-6 NSCLC xenograft model (IV-1602) (Report 4699-10)
- Effects of IMC-11 F8 in combination with Gemcitabine + Cisplatin on Gaussia luciferase expression in an A549-ciAP-GLuc NSCLC xenograft model (IV-1605) (Report 4702-10)
- Screen for additive effect of Lilly's IKKbeta inhibitor in an NCI-H1650 Non-Small Cell Lung Cancer Model treated with Gemcitabine + Cisplatin +/- IMC-11 FB (IV-1735) (Report 4832-10)
- Efficacy of IMC-11 F8 in combination with gemcitabine/cisplatin in a HOP-92 xenograft model of human NSCLC (IV-1779) (Report 4876-10)
- Efficacy of IMC-11 F8 in combination with Gemcitabine + Cisplatin in an NCI-H727 NSCLC xenograft model (IV-1847) (Report 4944-10)
- Efficacy of IMC-11 F8 ± gemcitabine/cisplatin in a xenograft model of NSCI-H226 human NSCLC (IV-1877) (Report 4974-10)
- Breakout Study of Mitomycin-C, IMC-11 F8 and CPT-11 in an HT-29 Xenograft Model (Report 4989-10)

- Breakout Study of Mitomycin-C, IMC-11 F8 and CPT -11 in an HCT -116 Xenograft Model (Report 4990-10)
- Synergy analysis of the combination of IMC-11 F8 and DC1 01 in a HCC827 human NSCLC xenograft model (Report 5086-11)
- Dose response of Erlotinib (Tarceva) and IMC-11 F8 in NCI-H1975 NSCL cancer xenograft model (IV-2006) (Report 5103-11)
- Add-on study of the Lilly Chk1-Inh II LY2940930 in combination with IMC-11 F8 and CPT -11 in the HT -29 colorectal cancer model (Report 5115-11)
- Add-on study of the Lilly Chk1-Inh II LY2940930 in combination with IMC-11 F8
- and CPT-11 in the HCT-116 colorectal cancer model (Report 5116-11)
- Efficacy of IMC-11 F8 in combination with Gemticitabine + Cisplatin, in JMSU1 bladder cancer xenograft model (IV-2030) (Report 5127-11)
- Efficacy of IMC-11 FS in combination with Gemticitabine + Cisplatin, in RT112 bladder cancer xenograft model (IV-2048) (Report 5145-11)
- Efficacy of IMC-F118 ± gemcitabine/cisplatin or ± carboplatin in a xenograft model of human RERF-LC-A1 squamous cell lung carcinoma (report 5308-12)
- Efficacy of IMC-A12 and IMC-11F8 in four A549 human lung adenocarcinoma KRAS variant cell lines (IV-2234) (Report 5331-12)
- Efficacy of IMC-F118 in combination with 5FU/cisplatin in a xenograft model of human NCI-N87 human gastric carcinoma (report 5358-12)
- Efficacy of IMC-F118 ± 5FU/cisplatin in a xenograft model of human SNU-5 human gastric carcinoma (IV-2262) (Report 5359-12)

Pharmacodynamic Drug Interactions

- Human anti-EGFR mAb IMC-11F8 efficacy in combination with irinotecan in GEO xenografts (Report 2111-03)
- IMC-11F8 dose-response with HT-29 xenografts (Report 2119-03)
- Human anti-EGFR mAb IMC-11F8 efficacy in combination with irinotecan in HT-29 colon carcinoma xenografts (Report 2120-03)
- Immunohistological analysis of human anti-EGFR mAb IMC-11F8 in combination with irinotecan in GEO colon carcinoma xenografts (Report 2215-03)
- Efficacy of human anti-EGFR mAb IMC-F118 and oxaliplatin on HT-29 xenografts (report 3596-06)
- Efficacy of human anti-EGFR mAb IMC-F118 and oxaliplatin on DLD-1 xenografts (report 3628-06)
- Efficacy of human anti-EGFR mAb IMC-F118 and oxaliplatin on GEO xenografts (report 3660-06)
- IMC-11F8 + gemcitabine/cisplatin combination therapy q7d in an A549 NSCLC xenograft model (IV-1221) (Report 4325-08)
- IMC-11F8 + gemcitabine/cisplatin combination therapy q7d in an NSI-H1650 NSCLC xenograft model (IV-1224) (Report 4328-08)
- Mechanism of action of IMC-11F8 in combination with gemcitabine and cisplatin in an A549 NSCLC xenograft model (IV-1331) (report 4430-09)
- Efficacy of IMC-11 F8 in combination with paclitaxel, in an A549 xenograft model (IV-1353) (Report 4452-09)

- Efficacy of IMC-11 F8 in combination with paclitaxel + Cisplatin, in an NCI-H1650 xenograft model (IV-1371) (Report 4468-09)
- Efficacy of IMC-11 F8 in combination with Gemcitabine+Cisplatin, Paclitaxel+Cisplatin or Pemetrexed+Cisplatin in an A549 NSCL cancer xenograft model (IV-1446) (Report 4543-09)
- Efficacy of IMC-11 F8 in combination with Gemcitabine+Cisplatin, Paclitaxel+Cisplatin or Pemetrexed+Cisplatin in an NCI-H1650 NSCLC xenograft model (IV-1447) (Report 4544-09)
- Efficacy of IMC-11 F8 in combination with Gemcitabine+Cisplatin, Paclitaxel+Cisplatin or Pemetrexed+Cisplatin in an NCI-H292 NSCL cancer xenograft model (IV-1484) (Report 4581-09)
- Efficacy of IMC-11 F8 in combination with Gemcitabine+Cisplatin, Paclitaxel+Cisplatin or Pemetrexed+Cisplatin in an NCI-H358 NSCL cancer xenograft model (IV-1486) (Report 4583-09)
- Efficacy of IMC-11 F8 alone or [in] combination with Pemetrexed+Cisplatin in an NCI-H1650 NSCLC xenograft model (IV-1524) (Report 4621-09)
- Efficacy of IMC-11 F8 in combination with Pemetrexed+Cisplatin in an A549 NSCLC xenograft model (IV-1525) (Report 4622-09a)
- Efficacy of IMC-11 F8 in combination with Gemcitabine+Cisplatin, Paclitaxel+Cisplatin, or Pemetrexed+Cisplatin in an NCI-H520 NSCL cancer xenograft model (IV-1548) (Report 4645-09)
- Efficacy of IMC-11 F8 in combination with Gemcitabine+Cisplatin, Paclitaxel+Cisplatin, or Pemetrexed+Cisplatin in an NCI-H441 NSCL cancer xenograft model (IV-1549) (Report 4646-09)
- Efficacy of IMC-11 F8 in combination with Gemcitabine+Cisplatin, Paclitaxel+Cisplatin, or Pemetrexed+Cisplatin in an HCC827 NSCL cancer xenograft model (IV-1550) (Report 4647-09)
- Efficacy of IMC-11 F8 in combination with Gemcitabine+Cisplatin, Paclitaxel+Cisplatin, or Pemetrexed+Cisplatin in an EKVX-P2 NSCLC xenograft model (IV-1603) (Report 4700-10)
- Efficacy of IMC-11 F8 in combination with Gemcitabine+Cisplatin, Paclitaxel+Cisplatin, or Pemetrexed+Cisplatin in an NCI-H1975 NSCLC xenograft model (IV-1604) (Report 4701-10)
- To determine [the] mechanism of action of IMC-11F8 in combination with gemcitabine and cisplatin in a xenograft model of NCI-H1650 human NSCLC (IV-1708) (Report 4805-10)
- Mechanism of action of IMC-11F8 in combination with gemcitabine + cisplatin in an A549 NSCLC xenograft model (IV-1709) (Report 4806-10)
- Efficacy of IMC-11 F8 in combination with Gemcitabine+Cisplatin in a HOP62 NSCLC xenograft model (IV-1780) (Report 4877-10)
- Efficacy of IMC-11F8 (anti-EGFR) and LY2875358 (anti-cMet) alone or in combination with gemcitabine + cisplatin in a HCC827 NSCLC xenograft model (IV-1818) (Report 4915-10)
- Efficacy of gemcitabine + cisplatin in combination with IMC-11F8 or IMC-A12 in an NCI-H1299 NSCLC xenograft model (IV-1819) (Report 4916-10)

- Efficacy of IMC-11F8 in combination with gemcitabine + cisplatin in HOP-92 NSCLC xenograft model (IV-1846) (Report 4943-10)
- Efficacy of IMC-11F8 in combination with gemcitabine + cisplatin in NCI-H2170 NSCL cancer xenograft model (IV-1873) (Report 4970-10)
- Efficacy of IMC-11F8 in combination with gemcitabine + cisplatin in NCI-H2405 NSCL cancer xenograft model (IV-1874) (Report 4971-10)
- To determine the efficacy of IMC-11F8 in combination with gemcitabine and cisplatin or gemcitabine + c-Met antibody (LY2875358) in NCI-H226 NSCL cancer xenograft model (IV-1875) (Report 4972-10)
- Efficacy of IMC-11F8 in combination with gemcitabine + cisplatin, in NCI-H647 NSCLC cancer [sic] xenograft model (IV-1946) (Report 5043-11)
- Efficacy of IMC-11F8 ± c-Met inhibitor LY2801653 and gemcitabine/cisplatin in a xenograft model of NCI-H1975 human NSCLC (IV-2263) (Report 5360-12)

3.3 Previous Reviews Referenced

None

4 Pharmacology

4.1 Primary Pharmacology

Li et al. 2008[1]

The purpose of this paper was to examine the mechanism of action of the fully human anti-EGFR antibody IMC-11F8 (necitumumab), partially through comparison to the mechanism of action of the approved anti-EGFR antibody, cetuximab. The authors showed that soluble EGFR bound to immobilized IMC-11F8 or cetuximab with similar affinities (3.3 and 2.3 nM, respectively). Binding of IMC-11F8 to soluble EGFR domain III alone occurred at lower concentrations than those observed for the whole protein. Antibody binding of IMC-11F8 blocked the ligand binding site of EGFR and prevented binding of EGF. The authors went on to show that the EGFR epitopes recognized by IMC-11F8 and cetuximab are overlapping, though the electrostatic interactions between each of the antibodies with their respective epitopes vary widely. In addition, the authors state that the two antibodies adopt almost identical orientations upon binding to EGFR. Previous work by the same group (Li et al. 2005[2]) showed that binding of cetuximab prevented EGF binding to the binding site and prevented the conformation change in the receptor required for dimerization. Because of the overall similarities in epitope binding, IMC-11F8 is projected to prevent dimerization in the same way as cetuximab.

Figure 2: Mechanism of Inhibition of EGFR Activation by IMC-11F8 and by Cetuximab

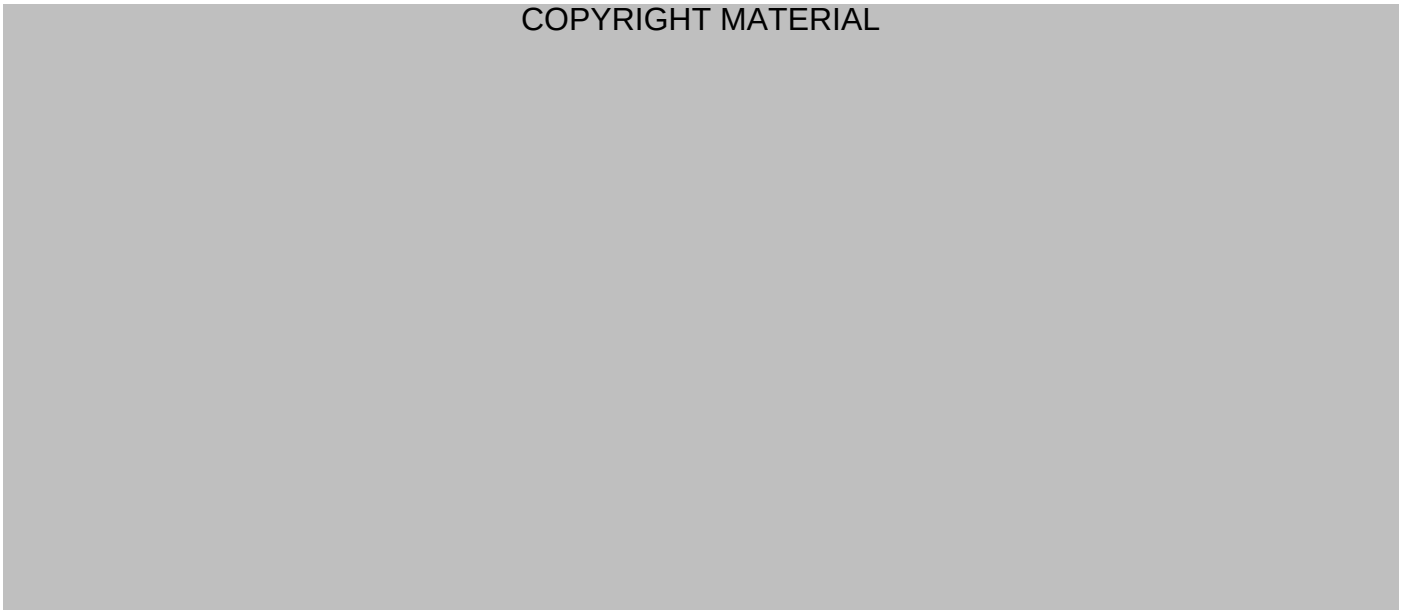

(Excerpted from Li et al. 2008)

4.1.1 Necitumumab (INC-11F8) Cross-Reactivity with Human ErbB2, ErbB3, and ErbB4 Receptors (Report #08-13-2013)

The purpose of this study was to assess the binding of necitumumab (IMC-11F8) to human ErbB2, B3 and B4 using an ELISA-based binding assay. Plates were coated with commercially-available recombinant ErbB-Fc conjugates, which consisted of N-terminal fusions between the extracellular domain of ErbB1, B2, B3 or B4 and the human IgG1 Fc. Coated plates were blocked then incubated with necitumumab and signal was detected with an HRP-conjugated secondary goat-anti-human IgG1 κ light chain polyclonal antibody.

As illustrated in Figure 3, necitumumab bound strongly to ErbB1 with an EC_{50} of ~15 pM, but did not bind to the extracellular domains of human ErbB2, B3 or B4 in this assay.

Figure 3: Binding of necitumumab to human ErbB receptors

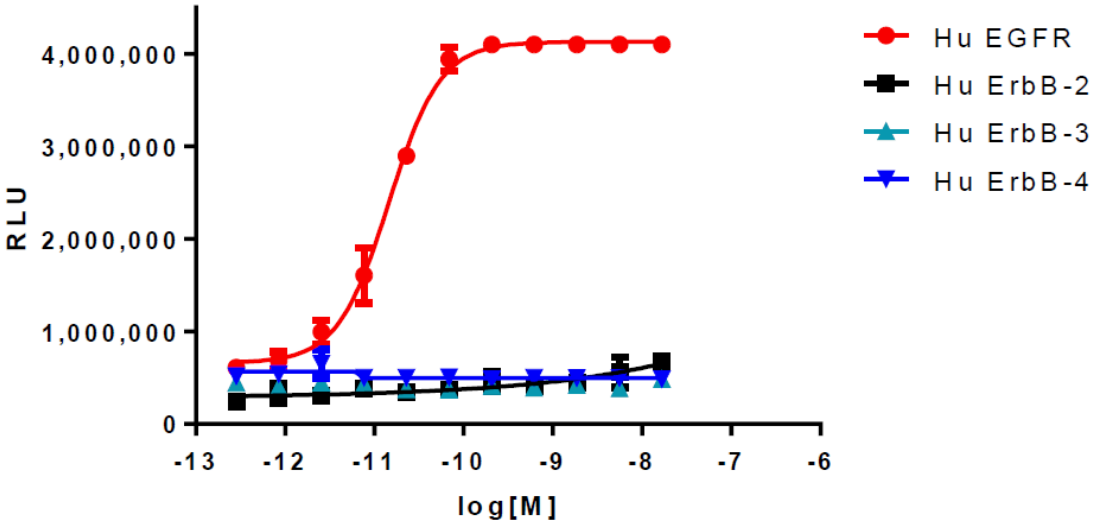

	Hu EGFR
EC50	1.455e-011

(Excerpted from the Applicant's BLA)

4.1.2 Efficacy of human anti-EGFR mAb C11F8 on A431 Epidermoid Carcinoma Xenografts (Report #1221-02)

The purpose of this study was to assess the ability of C11F8 (necitumumab) to inhibit the growth of A431 epidermoid carcinoma xenografts in an athymic nude mouse (nu/nu) model. $2X10^6$ tumor cells were injected into athymic nu/nu mice and allowed to grow until masses reached 200 mm^3. Treatment consisted of IP injections of either saline, Eribtux or necitumumab every 3 weeks for 6 weeks. Tumors were measured twice weekly (Q3D). As illustrated in Figure 4, there was a dose-dependent suppression of tumor growth with both necitumumab and Erbitux. At doses of 0.3 mg/kg Q3D, tumor growth in either antibody-treated group was approximately half of what was observed in controls. Tumor growth in animals treated with 1 mg/kg of either antibody was completely suppressed by the end of the dosing interval. Erbitux and necitumumab exhibited similar anti-tumor activity in this assay.

Figure 4: Anti-tumor response in nude mouse A431 xenografts following treatment with necitumumab or Erbitux

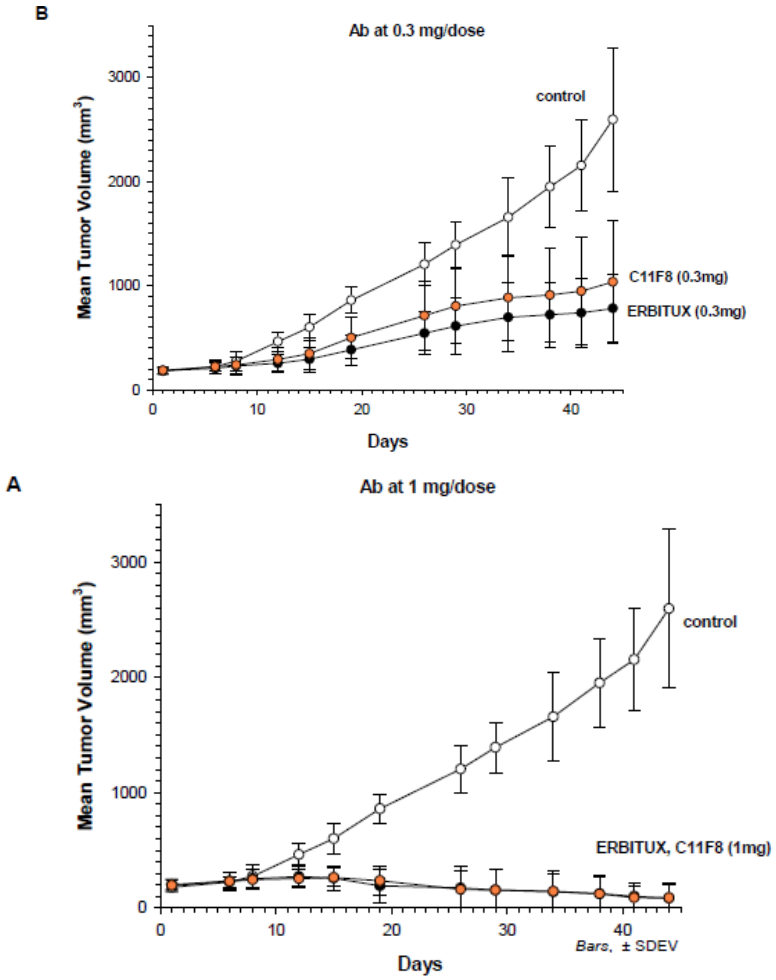

(Excerpted from the Applicant's BLA)

4.1.3 Efficacy of anti-IGF-IR mAb A12, Comparison of "Corn" (IMC-001) and Human (IMC-11F8) anti-EGFR mAbs to Cetuximab in BxPC-3 Human Pancreatic Xenografts (Report #1300-02)

This study compared the activity of 4 monoclonal antibodies, necitumumab (IMC-11F8, dosed at 0.3 and 1 mg/dose), an anti-IGF1R mAb (A12, dosed at 1 mg/dose; data not shown), a non-glycosylated anti-EGFR antibody(IMC-001, dosed at 0.3 or 1 mg/dose), and cetuximab (dosed at 0.3 or 1 mg/dose) in athymic mice implanted with BxPC-3 pancreatic carcinoma tumors. The Applicant did not provide the EGFR status of BxPC-3; however, it has been reported in the literature that this line expresses high levels of EGFR (Ali, et al., 2005). Animals were injected with $2X10^6$ BxPC-3 pancreatic carcinoma cells, and treatment commenced when tumors reached 200 mm^3. Antibodies were administered by intraperitoneal (IP) injection every 3 days for 7 weeks.

As indicated in Figure 5, anti-EGFR mAbs inhibited the growth of BxPC-3 tumors in a nude mouse model. The Applicant does not indicate whether the non-glycosylated antibody recognizes the same epitope as IMC-11F8, or whether it possesses effector functions (many aglycosylated antibodies do not). As these parameters were not discussed, it is difficult to interpret the mechanism by which the aglycosylated isoform mediated its anti-tumor activities (for example, by blocking receptor function or by mediating cell-killing).

Figure 5: Inhibition of BxPC-3 tumors by anti-EGFR mAbs

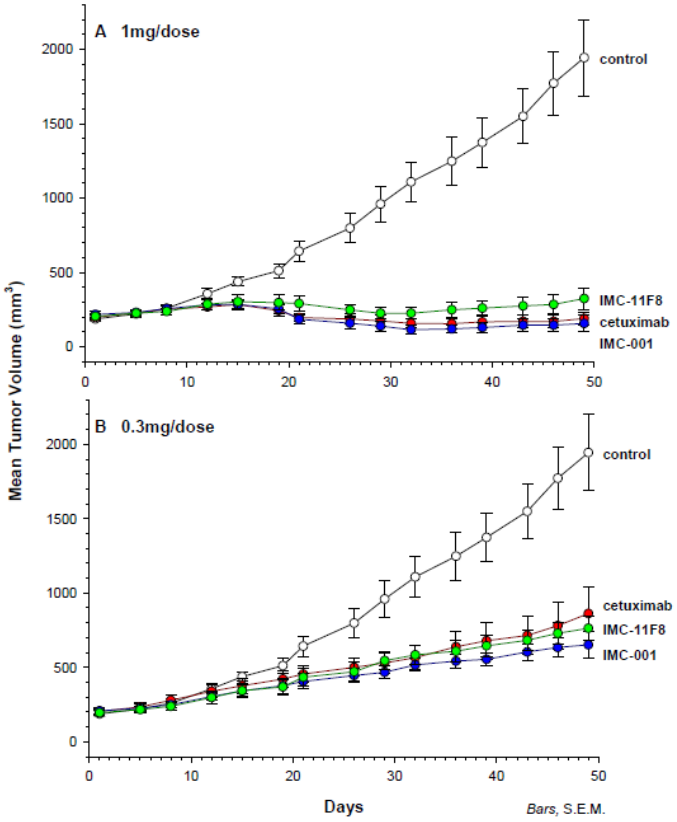

(Excerpted from the Applicant's BLA)

The Applicant also attempted to correlate tumor growth suppression with makers of tumor growth (pAKT and Ki67), apoptosis (cleaved caspase-3) and vascularity (pan endothelial cell marker); however, the results were too variable to inform the mechanism of action, or to provide potential biomarkers for clinical use.

4.1.4 Necitumumab-mediated internalization and degradation of EGFR-eGFP (Report #2013-8-15)

The purpose of this study was to determine if IMC-11F8 binding stimulates internalization of EGFR by tumor cells. To address this question, the Applicant constructed a C-terminal fusion of green fluorescent protein (GFP) to EGFR and overexpressed this construct in HELA cells. Cells were exposed in culture to IMC-11F8, and were evaluated using live cell confocal microscopy to assess the distribution of the EGFR label subsequent to antibody binding. The results obtained with IMC-11F8 were

compared with those obtained in cultures exposed to another anti-EGFR mAb (panitumumab).

Prior to mAb treatment, the fluorescence pattern was largely localized to the cellular periphery, consistent with distribution to plasma membrane. At 90 minutes post-treatment, cells exposed to a fluorescently-labeled IMC-11F8 (Denoted IMC-11F8-Alexa647) were observed to exhibit a punctate intracellular accumulation of GFP that co-localized with the Alexa647 label, suggesting that binding of IMC-11F8-Alexa647 mediated receptor internalization into the lysosomal compartment.

Figure 6: EGFR-GFP internalization following treatment with IMC-11F8

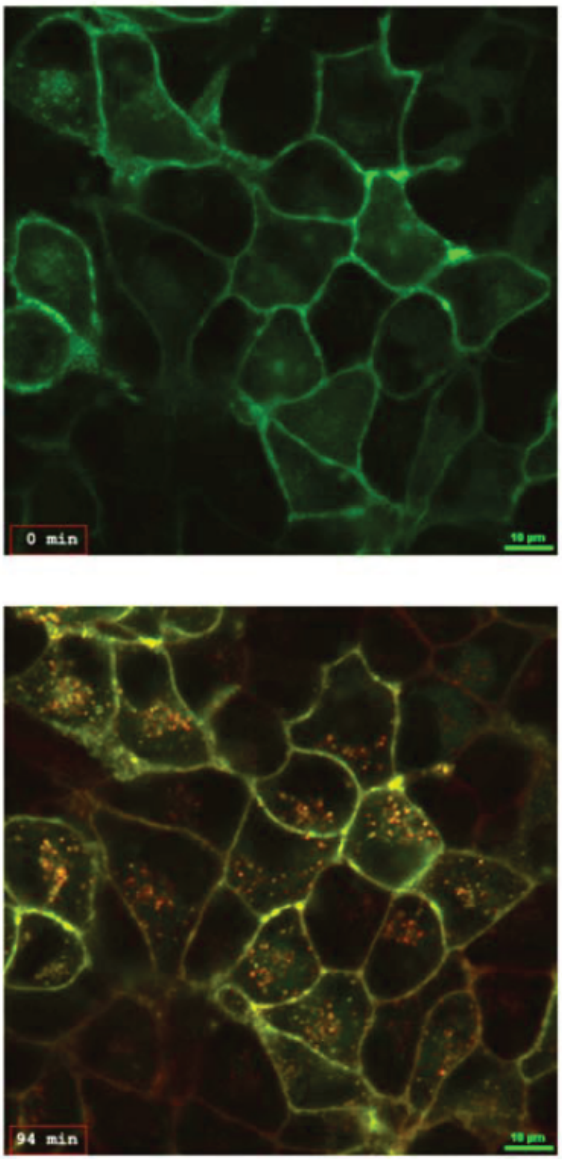

(Excerpted from the Applicant's BLA)

To determine the fate of the internalized receptor-antibody complex, the Applicant monitored the pixel intensity of the EGFR-GFP signal for 24 hours and observed a net decrease in signal intensity in cells cultured with IMC-11F8 over the observation interval, a finding that was not observed in cells cultured with an isotype control antibody (anti-KLH). Quantification of the GFP signal by flow cytometry confirmed a time-dependent decrease in EGFR-GFP over the 48-hour incubation period (Figure 7). The magnitude of this effect was compared with that of a competitor EGFR inhibitor (panitumumab). Though both IMC-11F8 and panitumumab were capable of mediating internalization, IMC-F118 was a more potent mediator of receptor internalization in this assay (Figure 8).

Figure 7: Quantification of GFP signal by flow cytometry

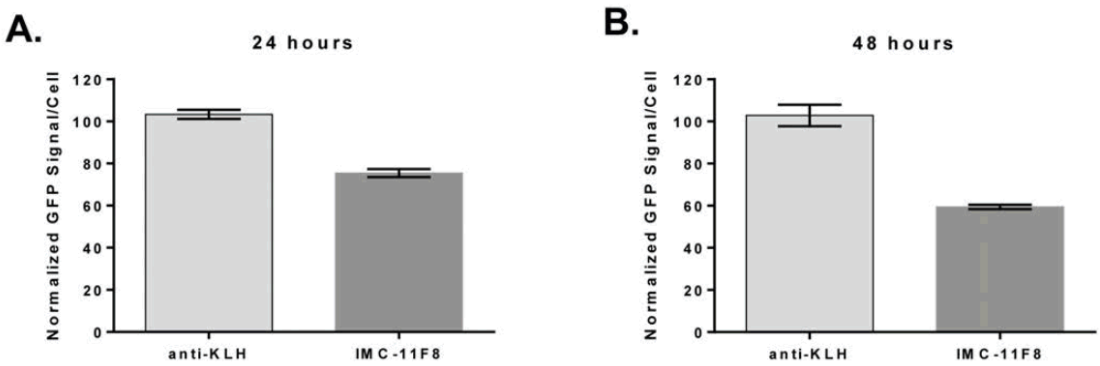

(Excerpted from the Applicant's BLA)

To confirm the lysosomal distribution of GFP-EGFR following treatment with IMC-11F8, EGFR-GFP-expressing cultures were treated with a Fab-anti-human IgG protein tagged with a dye that fluoresces at low pH (lysosomes). As illustrated in Figure 8 (left panel), IMC-11F8 treatment was associated with an increase in lysosomal fluorescence compared with isotype control or with panitumumab treatment. IMC-11F8 treatment was also associated with a decrease in the GFP signal over time, consistent with lysosomal degradation of the EGFR-GFP construct following IMC-11F8-mediated internalization (Figure 8, right).

Figure 8: Lysosomal localization (A) and degradation (B) of EFGR-GFP following treatment with IMC-11F8, panitumumab or isotype control mAb

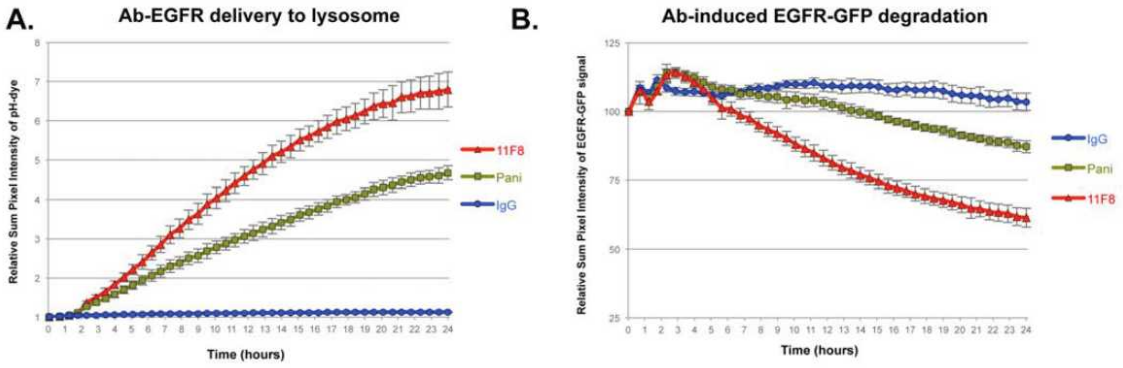

(Excerpted from the Applicant's BLA)

4.1.5 Species cross-reactivity of monoclonal anti-EGFR antibodies (cetuximab, necitumumab, panitumumab and ME-1) (Report #2013-9-10)

The purpose of this study was to determine the binding of anti-EGFR monoclonal antibodies to EGF receptors from potential toxicology species using an ELISA-based method. Briefly, 96-well plates were coated with recombinant soluble EGFR extracellular domain (ECD) proteins from human, cynomolgus monkey, mouse, rabbit and rat. Species-relevant ECDs were conjugated to either histidine tags or human Fc fragments. The specific constructs used, and their determined binding affinities, are provided in Table 2. As indicated, the binding affinity for EGFR ECD is comparable between human and cyno. Lower affinities were achieved against rodent and rabbit isoforms.

Table 2: EGFR ECD constructs used in species specificity assay

ECD Source	Construct	Necitumumab EC50	Cetuximab EC_{50}
Human	EGFR-ECD (Domains 1-4)	7.30 pM	11.7 pM
Human	EGFR-ECD-His	6.66 pM	8.81 pM
Cyno	EGFR-ECD-His	5.93 pM	8.44 pM
Mouse	EGFR-ECD-Fc	~ 20 nM	Not evaluated
Rabbit	EGFR-ECD-His	2.24 nM	7.00 pM
Rat	EGFR-His	~ 20 nM	Not evaluated

4.1.6 Inhibition of ligand-induced EGFR phosphorylation by necitumumab in LK-2 human squamous cell lung cancer cells stably expressing wild-type human EGFR (Report #2014-03-05)

The purpose of this study was to demonstrate that necitumumab blocks activation (as measured by phosphorylation) of EGFR in cultured LK2 cells by inhibiting the binding of EGFR to its ligands (human recombinant amphiregulin, betacellulin, EGF, epigen, epiregulin, HB-EGF, and TGFα). Cultured cells were exposed to EGF ligands at concentrations of 100 nM for 10 minutes, after which cells were lysed and pEGFR was measured by Luminex®. All of the ligands tested induced pEGFR. With the exception of Epigen, which demonstrated low baseline EGFR-activation in this assay, necitumumab potently inhibited all EGF-ligand induced pEGFR formation, with IC_{50}s of between 3.5 fM-74 nM (Figure 9).

Figure 9: Inhibition of Ligand-induced pEGFR by necitumumab in LK-2 WT EGFR cells

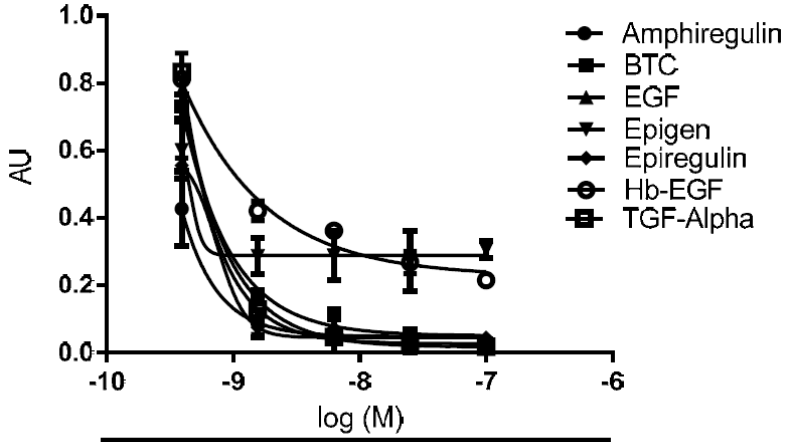

IC_{50}	Amphiregulin	1.812e-011
	Betacellulin (BTC)	6.040e-013
	EGF	9.550e-012
	Epigen	-
	Epiregulin	7.396e-010
	HB-EGF	3.554e-015
	TGF alpha	4.830e-012

(Excerpted from the Applicant's submission)

4.1.7 Effect of necitumumab, a fully human monoclonal antibody against the human epidermal growth factor receptor, on viability of DiFi and NCI-H508 human colon carcinoma cells (Report #2014-03-06)

The purpose of this study was to evaluate the effect of necitumumab on the viability of cultured DiFi and NCI-H508 cells, and to compare its effects with those of cetuximab. Cells were plated into 96-well plates and incubated with dilutions of IMC-11F8 (necitumumab) or IMC-C225 (cetuximab). After 72 hours, cells were incubated with Cell Titer-Glo reagent, which generates a luminescent signal in proportion to the ATP content of the culture. As indicated in Figure 10, necitumumab inhibited the viability of both NCI-H508 and DiFi colon carcinoma cells, and its activity was comparable to cetuximab in this assay.

Figure 10: Effect of necitumumab and cetuximab on viability of cultured DiFi and NCI-H508 cells

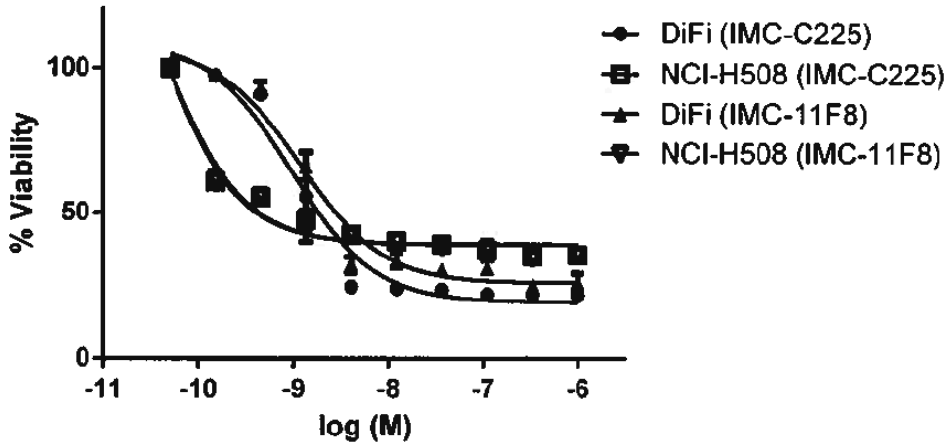

	DiFi (IMC-C225)	NCI-H508 (IMC-C225)	DiFi (IMC-11F8)	NCI-H508 (IMC-11F8)
IC50	9.700e-010	2.940e-011	1.206e-009	3.765e-011

(Excerpted from the Applicant's submission)

4.1.8 BxPC-3 #4EC PK/PD Study for IMC-11F8 Against BxPC-3 Xenografts (Report #2201-03A)

The purpose of this study was to evaluate the effect of necitumumab in a nude mouse pancreatic adenocarcinoma xenograft model. Female nu/nu mice received a single loading dose of 16.6, 55 or 166.2 mg/kg (for the low, mid and high dose level, respectively), followed by twice weekly doses of 0, 6, 20, or 60 mg/kg IMC-11F8 by IP injection for 5 weeks.

Tumor measurements were performed and plasma samples were collected for PK-PD assessments. Tumor growth was suppressed in a dose- and concentration-dependent fashion (Figure 11). Trough concentrations were 40, 100 and 465 µg/mL for the 6, 20 and 60 mg/kg dose levels, respectively, indicating overall dose-proportionality. Peak plasma exposures (115, 510 and 1440 µg/mL) were similarly proportional with dose over the range evaluated; however, given the low number of animals evaluated (1-2 per group and timepoint), it is not possible to assess the variability of the estimates.

Figure 11: Tumor growth inhibition (upper) and concentration-time profiles (lower) in pancreatic carcinoma xenografts treated with necitumumab

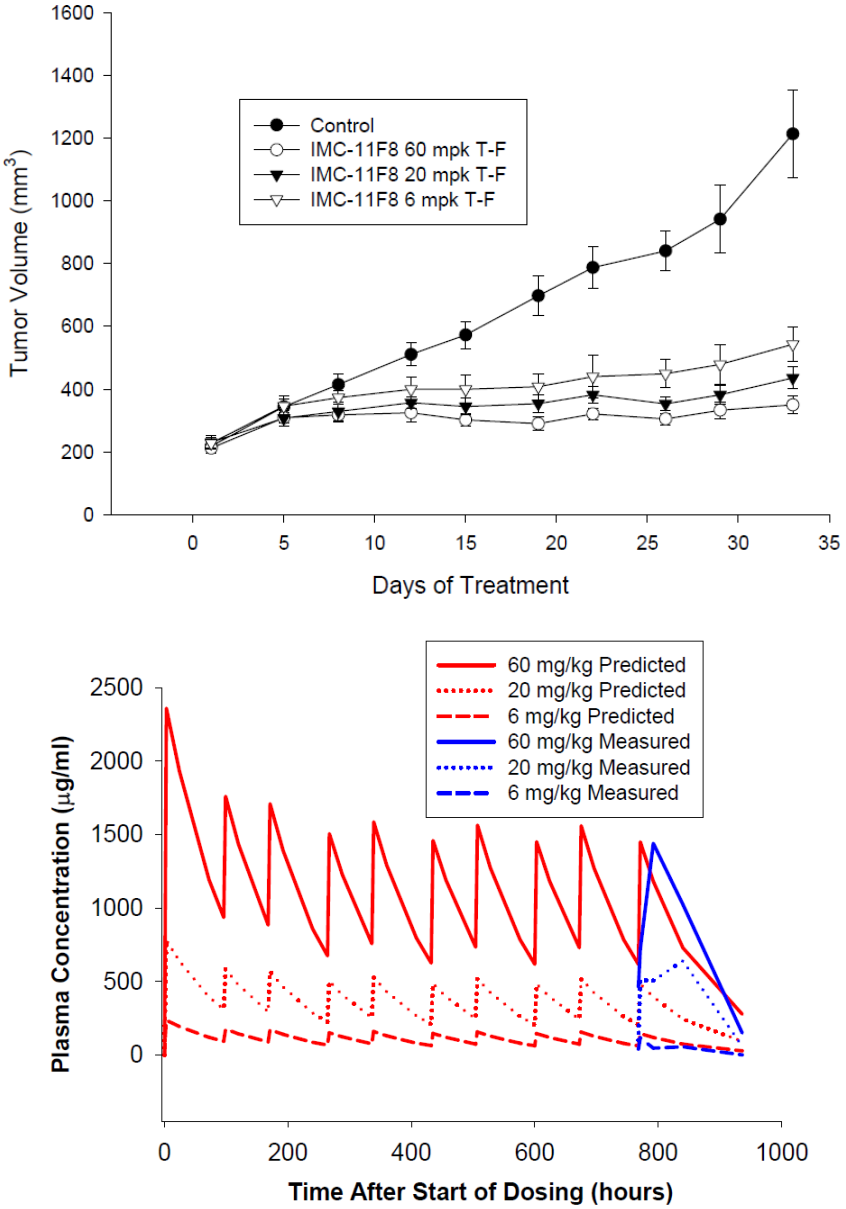

(Excerpted from the Applicant's BLA)

4.1.9 GEO #13: Comparison of human anti-EGFR mAb IMC-11F8 and cetuximab on GEO xenografts (Report #3708-06)

The purpose of this study was to evaluate the activity of necitumumab and cetuximab in a murine xenograft model using the EGFR-expressing (Kras-mutant) GEO human colorectal cancer cell line. Tumor-bearing animals received either cetuximab or necitumumab three times a week at doses of 1 mg/dose by intraperitoneal injection. As

indicated in Figure 12, the two drugs exhibited comparable anti-tumor activity in this model.

Figure 12: Growth of GEO tumors in mice treated with necitumumab or cetuximab

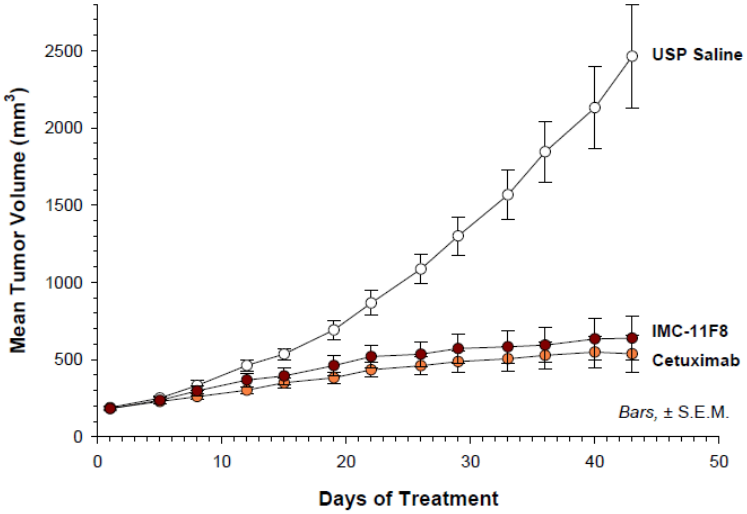

(Excerpted from the Applicant's BLA)

4.1.10 NCI-H292 #7PS: Efficacy study with monoclonal antibody IMC-11F8 (anti-EGFR) in a subcutaneous human NCI-H1975 non-small cell lung cancer (NSCLC) xenograft model (Report #3732-06)

The purpose of this study was to assess the anti-tumor activity of necitumumab in murine xenografts harboring human NCI-H1975 (EGFR activation mutant positive) non-small cell lung cancer tumors. Female nude (nu/nu) mice were implanted with $1X10^7$ NCI-H1975 cells SC and tumors were allowed to grow to a size of 201 mm^3 prior to treatment with either IMC-11F8 (0.4-40 mg/kg) or saline. Antibodies were administered by the IP route twice weekly. As illustrated in Figure 13, treatment with IMC-11F8 inhibited the growth of tumors in this model at all doses tested.

Figure 13: Response of NCI-H1975 xenografts to IMC-11F8

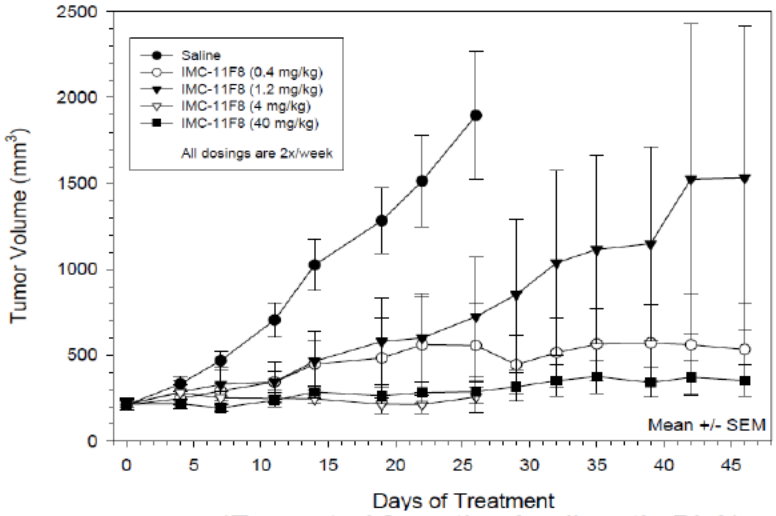

(Excerpted from the Applicant's BLA)

4.1.11 NCI-H292 #7PS: Efficacy study with monoclonal antibody IMC-11F8 (anti-EGFR) in a subcutaneous human NCI-H292 non-small cell lung cancer (NSCLC) xenograft model (Report #3733-06)

The purpose of this study was to assess the anti-tumor activity of necitumumab in murine xenografts harboring human NCI-H292 (wt-EGFR) non-small cell lung cancer tumors. Animals received either 0.4, 1.4, 4 or 40 mg/kg necitumumab twice weekly by intraperitoneal injection for 38 days. As indicated in Figure 14, all doses of necitumumab were active in this model, with maximal activity observed at doses of ≥ 4 mg/kg twice weekly.

Figure 14: Effect of necitumumab in NSCLC xenografts

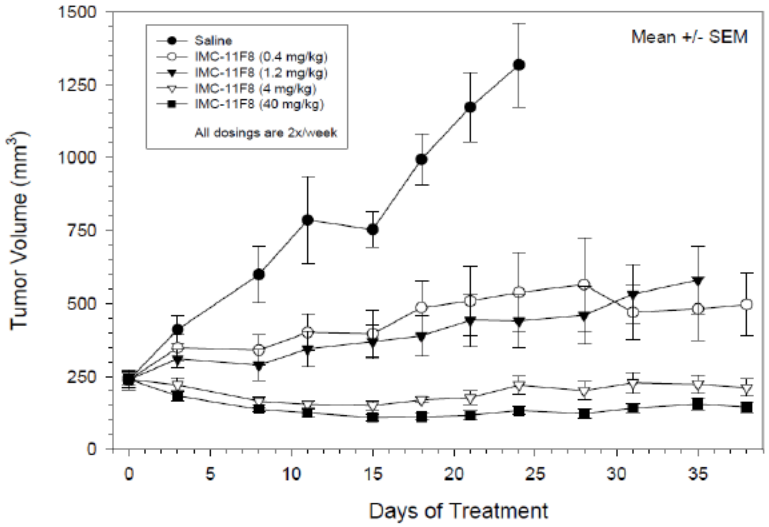

(Excerpted from the Applicant's BLA)

4.1.12 HCC827#1EC: PK/PD of IMC-11F8, cetuximab, and panitumumab in a HCC827 NSCLC xenograft model (Report #4983-10)

The purpose of this study was to evaluate the effect of necitumumab (IMC-11F8) in comparison to cetuximab or panitumumab in a murine model of NSCLC and to correlate anti-tumor activity with plasma exposures. Animals received 0.06, 0.6 or 6 mg/kg of necitumumab, panitumumab or cetuximab by IP injection twice weekly. The first dose was a loading dose of 2.5X the maintenance dose. Tumor volume was measured twice weekly through day 34.

As illustrated in Figure 15, all regimens were equally active in this model. Moreover, as illustrated in Figure 16, plasma exposures were comparable between necitumumab and panitumumab.

Figure 15: Dose-response of necitumumab, cetuximab or panitumumab in a murine model of NSCLC

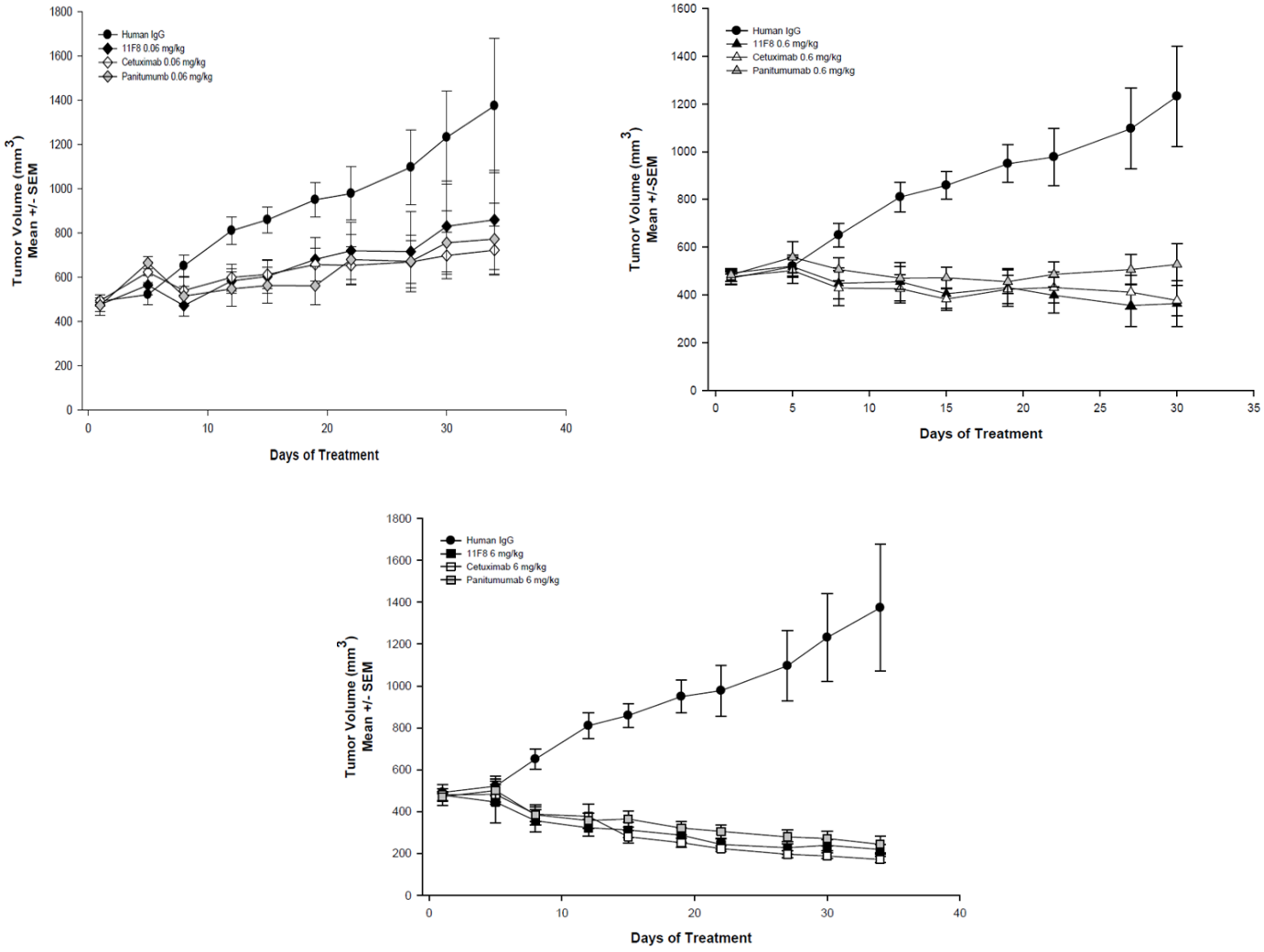

(Excerpted from the Applicant's BLA)

Figure 16: Individual plasma concentrations for necitumumab and panitumumab in the murine NSCLC efficacy model

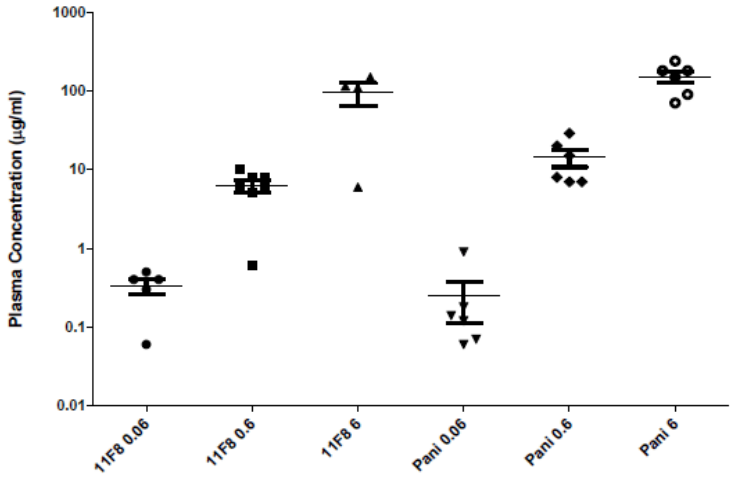

(Excerpted from the Applicant's BLA)

4.1.13 NCI-H441#1HL: Efficacy of IMC-11F8 (necitumumab) in NCI-H441 NSCLC xenografts stably overexpressing wild type EGFR (IV-2130); (Report #5227-11)

The purpose of this study was to evaluate the effect of necitumumab in a murine model implanted with a NSCLC xenograft that stably-overexpressed WT EGFR. Nude mice (nu/nu) were injected with $1X10^7$ NCI-H441 cells and tumors were allowed to grow until an average volume of 350 mm^3, at which time, animals were randomized to receive either saline or necitumumab twice weekly by IP injection. As illustrated in Figure 17, high-dose necitumumab (60 mg/kg) exhibited activity in this model, suggesting that the drug exhibits activity against endogenous EGFR.

Figure 17: Activity of necitumumab in a murine model of NSCLC that stably overexpressed WT EGFR

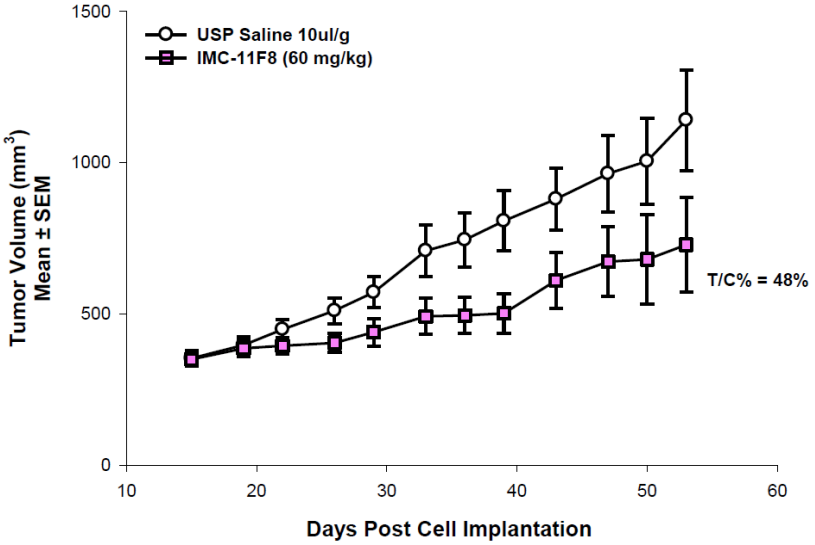

(Excerpted from the Applicant's BLA)

4.1.14 NCI-H441#3HL: Efficacy of necitumumab (IMC-11F8) in NCI-H441 NSCLC xenografts stably overexpressing mutated (Δ746-750) EGFR (IV-2132); (Report #5229-11)

The purpose of this study was to evaluate the effect of necitumumab in a murine model implanted with a xenograft that stably-overexpressed mutant (Δ746-750) EGFR. Twice-weekly IP doses of necitumumab (60 mg/kg) exhibited weak activity in this model.

The Applicant does not comment on the relatively poor response observed in mutant-EGFR-over-expressing H441 cells compared with activity in other, spontaneously-mutant lines (e.g. HCC827).

Figure 18: Activity of necitumumab in a murine model of NSCLC that stably overexpressed mutant (Δ746-750) EGFR

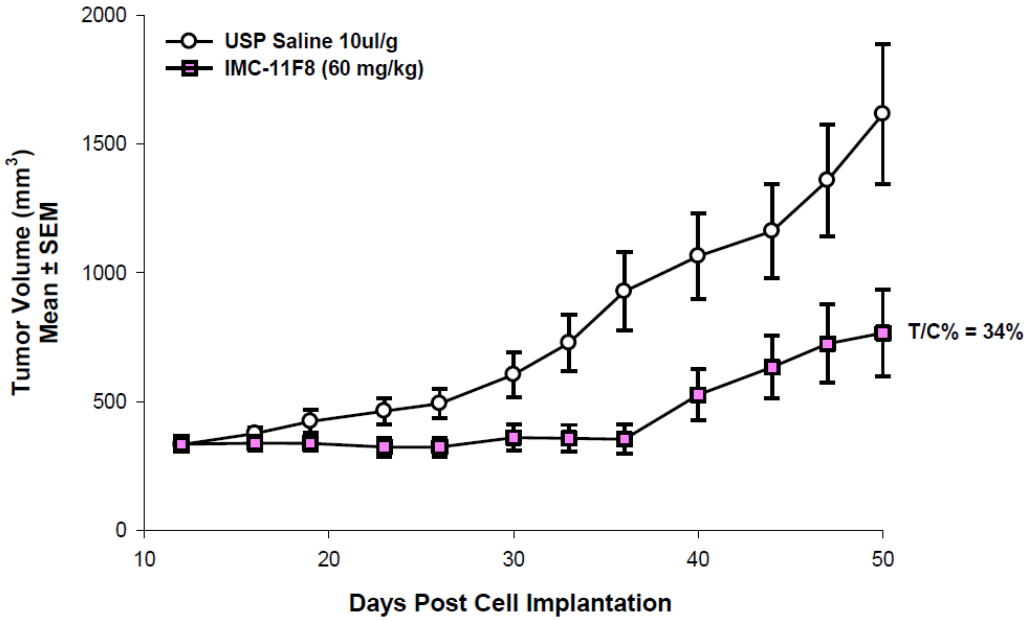

(Excerpted from the Applicant's BLA)

4.1.15 NCI-H441#4HL: Efficacy of IMC-11F8 (necitumumab) in a SC xenograft model of NCI-H441 human NSCLCEGFR (IV-2152); (Report #5249-11)

The purpose of this study was to evaluate the effect of necitumumab in a murine model implanted with an untransfected NCI-H441 NSCLC xenograft. Necitumumab was administered twice weekly at a dose of 60 mg/kg by the IP route. Tumor volumes were measured twice weekly during the dosing interval. There was no activity of necitumumab in this model Figure 19.

Figure 19: Activity of necitumumab in the NCI-H441 tumor model

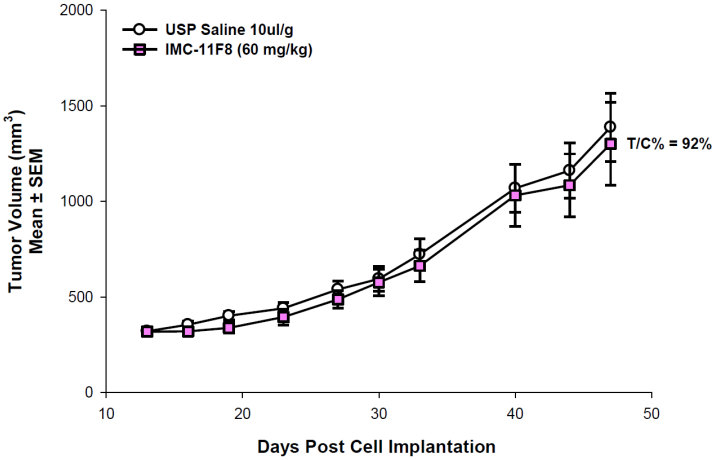

(Excerpted from the Applicant's BLA)

4.1.16 Generation and preclinical characterization of the fully-human anti-EGFR monoclonal antibody IMC011F8; (Report #IMC11F8-01)

This report describes the construction and characterization of necitumumab, a fully human anti-EGFR mAb. A series of studies were performed to characterize its binding and pharmacodynamic properties, including binding to recombinant human EGFR (rhEGFR) by ELISA in comparison with cetuximab; EGFR binding by Biacore®; inhibition of EGFR-dependent cellular proliferation; in vitro ADCC; and in vivo tumor growth inhibition.

As illustrated in Figure 20, the binding kinetics between necitumumab and cetuximab were comparable in this assay.

Figure 20: Binding of EGFR by necitumumab or cetuximab as measured by ELISA

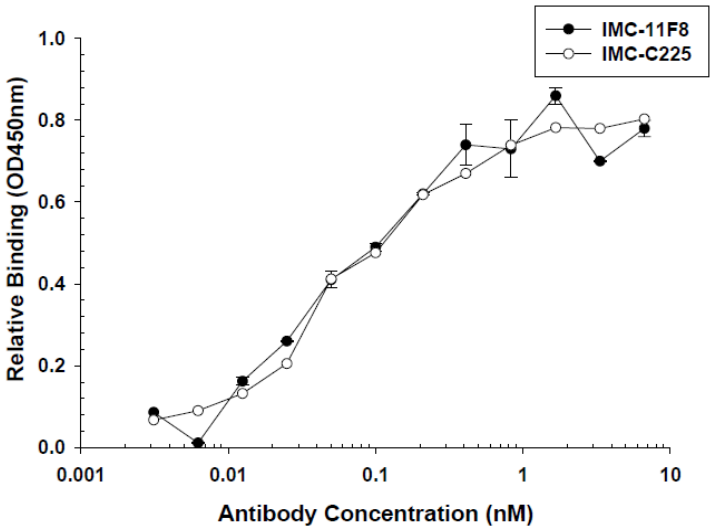

(Excerpted from the Applicant's BLA)

Pre-incubation of A431 cells (a human EGFR-overexpressing squamous cell carcinoma cell line) with necitumumab inhibited ^{125}I-EGF-labeled EGF - receptor binding, as demonstrated in Figure 21. This effect could be reversed by addition of unlabeled EGF (positive control), indicating that necitumumab effectively blocked binding of ^{125}I-EGF in this assay. No inhibition was observed when cells were treated with isotype (negative) control mAb.

Figure 21: Inhibition of ^{125}I EGF binding in A431 cells compared with unlabeled EGF (positive control) and isotype control mAb (negative control)

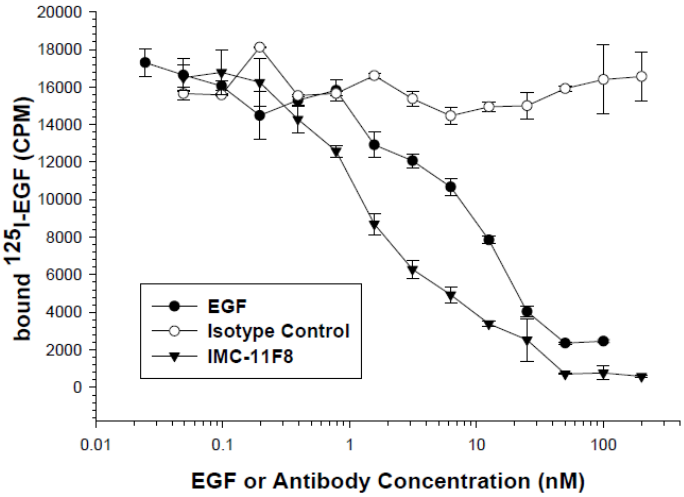

(Excerpted from the Applicant's BLA)

Similarly, pre-incubation of A431 cells with necitumumab or cetuximab inhibited phosphorylation of EGFR (Figure 22) and to a lesser degree, inhibited phosphorylation of p44/42 MAPK (Figure 23). Similar results were obtained in HT-29 and BxPC-3 cells (data not shown).

Figure 22: Inhibition of EGF-induced EGFR phosphorylation in A431 cells

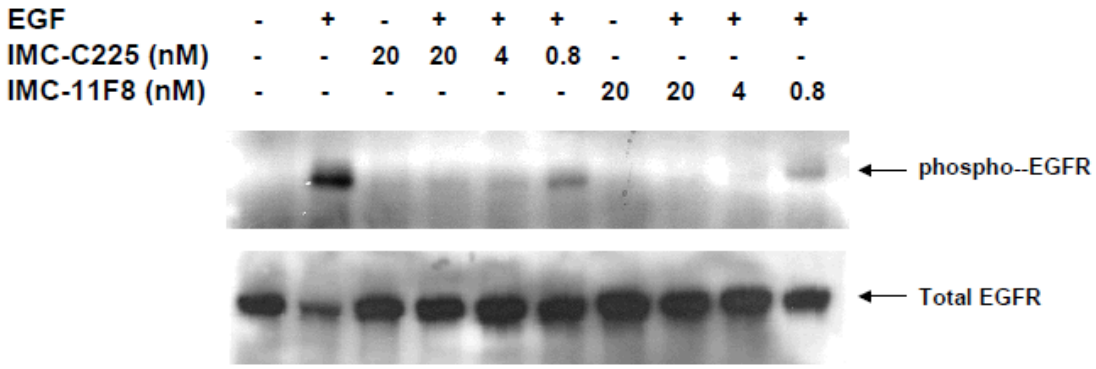

(Excerpted from the Applicant's BLA)

Figure 23: Inhibition of EGF-induced p44/42 MAPK phosphorylation in A431 cells

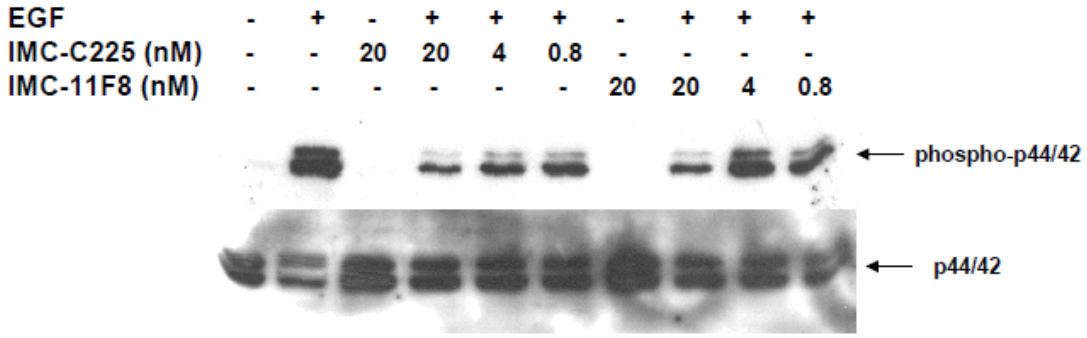

(Excerpted from the Applicant's BLA)

In cultured DiFi colon carcinoma cells, treatment with either necitumumab or cetuximab for 96 hours reduced the numbers of cells in the assay [as measured by mitochondrial MTT (3-(4,5-dimethylthiazol-2-yl)-2,5-diphenyltetrazolium bromide) conversion, the extent of which is proportional to cell viability and cell number]. Compared with an isotype control antibody, pretreatment with necitumumab or cetuximab decreased the MTT signal in EGF-stimulated cultures (Figure 24). Although they did not state whether they concurrently evaluated cell viability in these assays, the reduction in signal suggests that mechanism of MTT inhibition involved suppression of cell number in treated cultures through blockade of the EGF mitogenic signal.

Figure 24: Inhibition of DiFi colon carcinoma cell proliferation by necitumumab or cetuximab

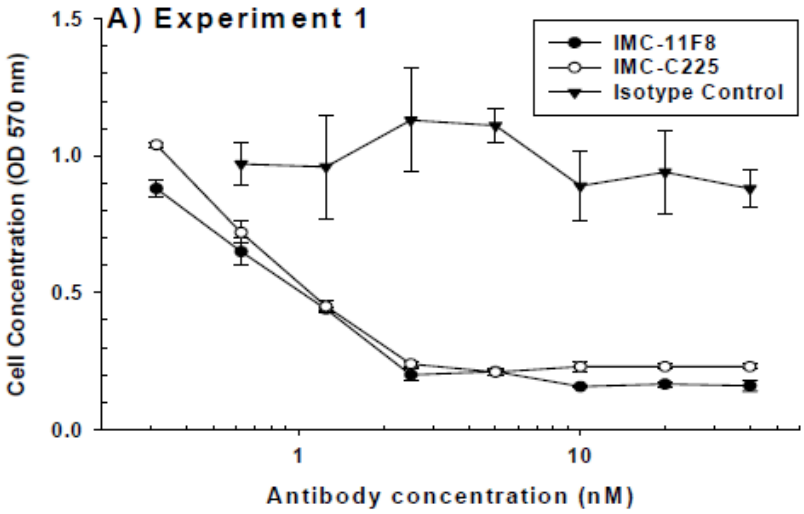

(Excerpted from the Applicant's BLA)

The Applicant also characterized the effector activity (ADCC) of necitumumab in cocultures of DiFi cells with primary cultured human PBMCs. When PBMCs were

incubated with EGFR-expressing DiFi colon cancer cells, necitumumab and cetuximab (50 µg/mL) both induced lysis of target tumor cells (Figure 25).

Figure 25 Necitumumab- or cetuximab-induced ADCC

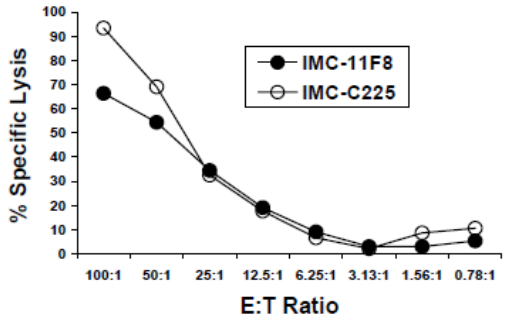

(Excerpted from the Applicant's BLA)

In vivo, administration of cetuximab or necitumumab induced tumor regression in nude mouse xenografts (A431 cells; N = 7-8 mice/group) when administered at twice-weekly doses of either 0.3 or 1 mg/dose (Figure 26). Similar results were obtained with the BxPC-3 (pancreatic) murine xenograft model (data not shown).

Figure 26: Inhibition of A431 tumors in nude mouse xenografts by cetuximab or necitumumab

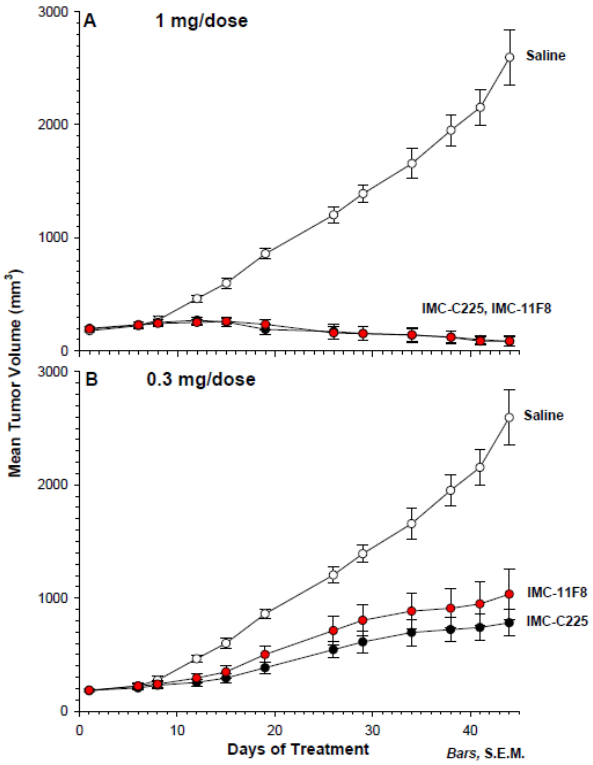

(Excerpted from the Applicant's BLA)

The Applicant demonstrated that necitumumab binds to tissues derived from human and cynomolgus monkeys. While the purpose of tissue-cross-reactivity studies is typically to demonstrate comparability of binding between nonclinical and clinical species, and to potentially identify patterns of drug-related toxicity, in this study, the Applicant chose to evaluate each tissue in only one species, and therefore, it is not possible to conclude that the binding pattern was similar between the two species (see Figure 27)

Figure 27: Binding of necitumumab to human or cynomolgus monkey tissues

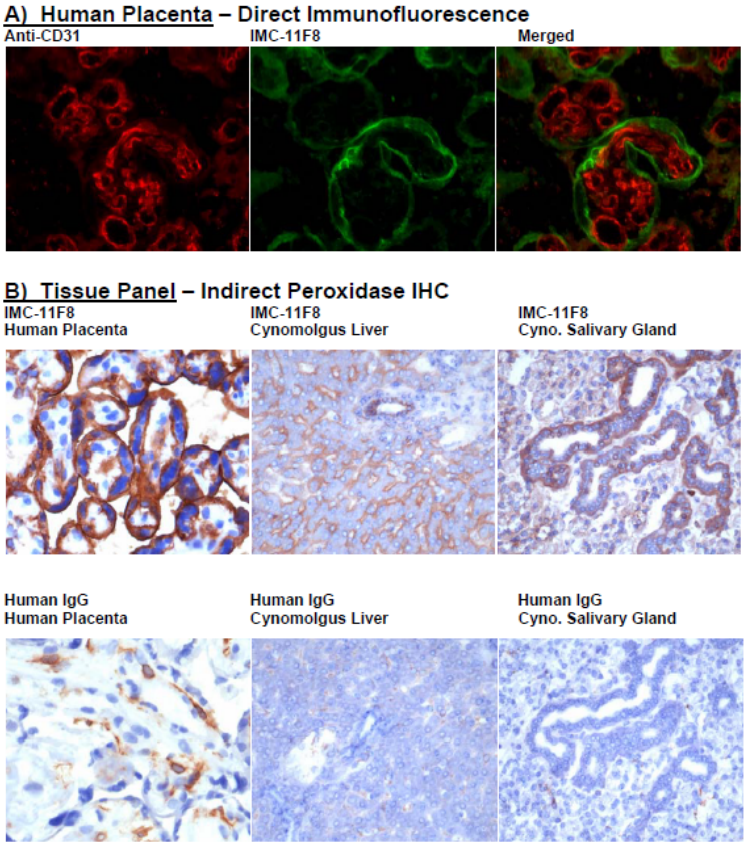

(Excerpted from the Applicant's BLA)

Finally, the Applicant evaluated the kinetics of necitumumab and cetuximab by surface plasmon resonance (Biacore). rhEGFR was immobilized on the sensor chip and binding kinetics were measured in solutions of cetuximab or necitumumab (either whole IgGs or FAbs) at concentrations of 1.5-100 nM. As illustrated in Table 3, the K_ds of cetuximab and necitumumab were highly comparable (0.32±0.05 vs 0.38±0.18 nM).

Table 3: Binding kinetics of necitumumab or cetuximab IgGs or Fabs as evaluated by surface plasmon resonance

Antibody		*kon* (10^5 $M^{-1}S^{-1}$)	*koff* (10^{-4} S^{-1})	Kd (nM)
IMC-11F8	Fab	22.9 ± 9.9	36.7 ± 8.5	1.78 ± 0.51
	IgG	20.8 ± 7.7	6.5 ± 2.2	0.32 ± 0.05
IMC-C225	Fab	23.1 ± 4.8	11.7 ± 3.4	0.53 ± 0.17
	IgG	18.2 ± 6.4	6.0 ± 1.1	0.38 ± 0.18

* All numbers are determined by BIAcore analysis and represent the mean ± SE from at least three separate determinations.

(Excerpted from the Applicant's BLA)

4.1.17 Investigation of Ramucirumab ADCC activity (Report #SDR-13049-00)

The purpose of this study was to evaluate the ability of ramucirumab and necitumumab to elicit ADCC against cell lines that express VEGFR2 (ramucirumab) and EGFR (necitumumab). The focus of this study was the ADCC activity of ramucirumab; necitumumab was added as a control. Only data from necitumumab studies will be discussed. To assess the potential for necitumumab to elicit ADCC, HCC827 cells were cultured overnight, then incubated in the presence of between 1 pM-1000 nM necitumumab for 1 hour followed by a 4-6 hour incubation with IL-2-stimulated effector cells. Lysis was assessed using a fluorometric LDH-quantification kit. As illustrated in Figure 28, necitumumab binds HCC827 cells and mediates ADCC in the presence of activated effector PBMCs. In addition, the Applicant performed a flow cytometry study and demonstrated that necitumumab bound PE-conjugated CD16a and EGFR simultaneously (data not shown).

Figure 28: ADCC assay (mean fluorometric LDH detection)

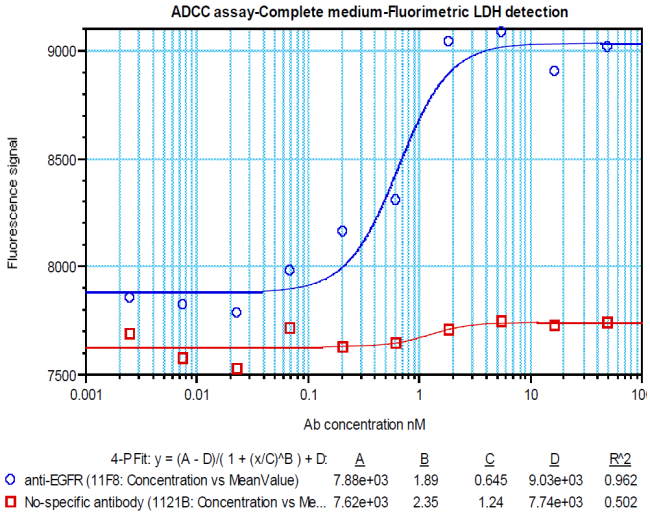

(Excerpted from the Applicant's BLA)

4.1.18 Efficacy of IMC-11F8 in combination with gemcitabine+cisplatin, paclitaxel,+cisplatin or pemetrexed+cisplatin in an A459 NSLC cancer xenograft model (IV-1446) (Report #4543-09)

The purpose of this study was to evaluate the effect of necitumumab (IMC-11F8) in combination with gemcitabine+cisplatin, paclitaxel+cisplatin or pemetrexed+cisplatin in an A459 NSCLC model in athymic mice.

$10X10^7$ A549 cells were injected SC into the left flank of female nude (nu/nu) mice and allowed to grow to a size of 300 mm^3, at which point, animals received one of these five treatments:

1. USP Saline 0.1ml per 10g body weight, M-Tu-F.
2. IMC-11F8 (60 mg/kg, Tu & F).
3. Cisplatin (3 mg/kg, q7d) + Gemcitabine (500 mg/kg, q7d) + IMC-11F8.
4. Paclitaxel (5 mg/kg, q7d x 3 weeks) + Cisplatin (5 mg/kg, q7d) + IMC-11F8.
5. Pemetrexed (100 mg/kg, 5 days a week, Monday through Friday for 2 weeks) + Cisplatin (5 mg/kg, q7d) + IMC-11F8.

As illustrated in Figure 29, all combinations were active in this model. While necitumumab exhibited antitumor activity, each of the combinations exhibited greater anti-tumor activity than necitumumab alone.

Figure 29: Inhibition of A549 NSCLC tumors in nude mouse xenografts by necitumumab in combination with cisplatin+gemcitabine, paclitaxel+cisplatin or pemetrexed+cisplatin

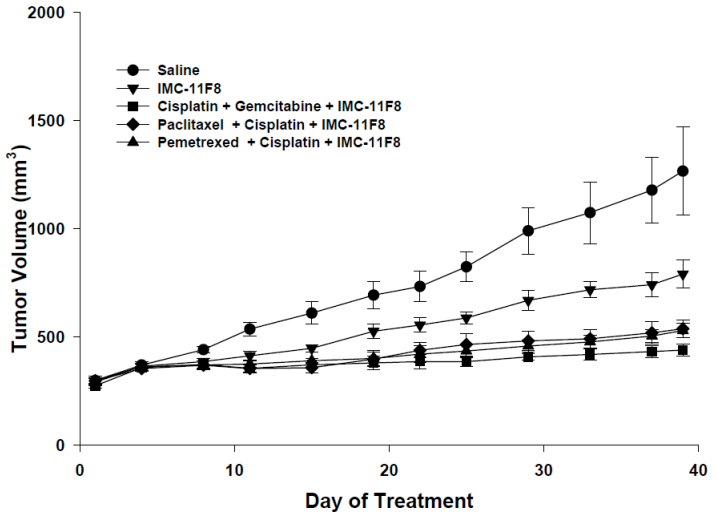

4.1.19 Mechanism of action of IMC-11F8 in combination with gemcitabine and cisplatin in an NCI-H1650 NSCLC xenograft model (IV-1329) (report 4428-09)

The purpose of this study was to evaluate the anti-tumor mechanisms of necitumumab (IMC-11F8) alone or in combination with cisplatin and gemcitabine, in an athymic

(nu/nu) murine model of NSCLC. Mice were implanted with $1X10^7$ NCI-H1650 cells and the tumor was allowed to grow to a size of 280 mm^3, at which point, animals commenced treatment with saline, IMC-11F8 (60 mg/kg T and F), gemcitabine+cisplatin (500 mg/kg gem; 3 mg/kg cis Q7D), or the triple-combination regimen.

On Day 9, 24 hours post-dose, 12 tumors/group were collected and fixed for histological evaluation of Meca-32, Ki-67, and Caspase 3 in order to measure angiogenic, proliferative, and apoptotic activities in tumor cores and at the periphery of the tumors. Tissues were also stained for hIgG1 to assess potential for IMC-11F8 tumor penetration, however, these data were not quantified.

The remaining 6 tumors/group were cut in half and flash frozen for RNA and micro-RNA isolation. The results of these analyses will not be discussed, as they were not clearly informative about the mechanism of action.

Staining for MECA32 demonstrated that the triple combination treatment reduced the number of meca-32-positive blood vessels at the tumor periphery and the blood vessel area in the tumor core (mean percentage of the visual field occupied by blood vessels) compared with either saline or necitumumab alone, but did not affect the density of blood vessels in the tumor periphery (mean number of vessels per square millimeter). Other parameters included a decrease in the number of Ki-67-positive cells in both the tumor periphery and the tumor core, and a decrease in the number of phosphor-histone-H3-positive cells in the tumor core and periphery.

Table 4: Summary of results from histological studies of murine (nu/nu) xenografts treated with necitumumab, gem/cis or the combination

Histological Parameter	Saline	Necitumumab	Gem/Cis	Combo
Blood vessel area (core)	2.02	1.98	1.23**, ‡	0.87**, §
Blood vessel area (periphery)	2.08	1.72	1.29**	0.94**, §
Blood vessel density (core)	63.85	54.82	53.02	51.67
Blood vessel density (periphery)	70.62	59.34	48.51**, †	64.44
% Ki-67 positive (core)	23.28	15.89	18.01	8.01**
% Ki-67 (periphery)	28.73	18.65**	15.26**	9.3**, §
% pHistone-H3 (core)	0.9	0.81	0.18**, ‡	0.06**, §
% pHistone-H3 (periphery)	1.04	0.95	0.11**, ‡	0.08**, §
% ApopTag-positive cells (core)	13.03	16.28	21.81	15.9
% ApopTag-positive cells (periphery)	11.77	15.92	19.11	13.47

** = Statistically significant vs. saline control

§ = necitumumab vs. combo Statistically significant r

‡ = necitumumab vs. Gem/Cis Statistically significant

† = Gem/Cis vs. combo Statistically significant

4.3 Safety Pharmacology

Not conducted

5 Pharmacokinetics/ADME/Toxicokinetics

5.1 PK/ADME

Study 7573-110: A multiple dose pharmacokinetic study of IMC-11F8 administered to cynomolgus monkeys (GLP compliant)

Findings:

- Pharmacokinetics of necitumumab manufactured using [redacted] (b) (4) appear to be comparable
- Immunogenicity results were difficult to interpret; the level of circulating serum IMC-11F8 concentrations may have interfered with the detection of anti-drug antibodies capable of binding to IMC-11F8.

Methods

Drug: IMC-11F8

Lot #	Manufacturing process	Target concentration of active ingredient	% Purity (assumed)
07C00265	[redacted] (b) (4)	[redacted] (b) (4) mg/mL	100
08T00297		[redacted] (b) (4) mg/mL	100

Dosing parameters: Drug administered D1, 22, and 29 via saphenous vein as10m infusion.

Process	ROA	Target dose (mg/kg)	Target dose concentration (mg/mL)	Target dose volume (mL/kg)
[redacted] (b) (4)	iv	12	1.2	10
	iv	12	1.2	10

Formulation: Saline dilution

Process	Active ingredient concentration (mg/mL)	Stock solution volume (mL)	Test article amount (mg)	Saline volume (mL)	Total volume (mL)
[redacted] (b) (4)					

Notes: Two dosing preparations were not analyzed due to fungal contamination.

[redacted] (b) (4)

Species/Strain: Cynomolgus monkey (drug naïve), 2.1-3.1 kg, 29-45 months old
Number/group: 10/sex/group

Observations

Parameter	Time of assessment
Mortality/clinical observation	1-2/day
Body weights	Prior to dosing + daily during dosing
PK sampling (~1.5 mL)	Prior to dosing, 0.25, 0.5, 1, 2, 4, 8, 12, 24,, 48, 72, and 96h post dose D1 and D7, 14, 21 at time of D1 dose administration
Immunogenicity sampling (~1.5 mL)	Prior to dosing D1 and D29, D38 at time of D29 dose administration

Monkeys were transferred to stock colony following immunogenicity and pharmacokinetic sampling collection

Observations

Parameter	[redacted] (b) (4) (12 mg/kg) M+F	[redacted] (b) (4) (12 mg/kg) M+F
Mortality/clinical observation	Liquid feces	Liquid feces
Body weights	UR	UR

Serum samples were analyzed using validated ELISA bioanalytical method.

In general, exposure to 12 mg/kg IMC-11F8 (necitumumab) was similar between drug substance [redacted] (b) (4) (see table and figures below). Mean half-life was ~88 hours for [redacted] (b) (4) in both gender, and ranged from 73 to 95 hours for [redacted] (b) (4) These half-life values are shorter than half-lives observed with some other monoclonal antibodies (~ 1 week). Concentrations were generally below the limit of quantitation by 312 hours. IMC-11F8 [redacted] (b) (4) lots appear to be pharmacokinetically similar in this assay.

Table 2: Comparative pharmacokinetic parameters of [redacted] (b) (4) lots

Dose Group	Sex		C_{max} (µg/mL)	T_{max} (hr)	$t_{1/2}$ (hr)	AUC_{0-480} (µg·hr/mL)	$AUC_{0-\infty}$ (µg·hr/mL)	Cl (mL/hr/kg)	V_z (mL/kg)
[redacted] (b) (4)									
(12 mg/kg)	M	Mean	418	3.50	88.5	25778	22613	0.532	56.8
		SD	102	4.21	29.4	6130	1400	0.032	5.6
	F	Mean	387	2.43	88.0	25350	25103	0.481	36.0
		SD	48	2.37	45.4	4164	2512	0.048	18.2
[redacted] (b) (4)									
(12 mg/kg)	M	Mean	389	2.30	73.5	22763	22752	0.532	56.2
		SD	142	3.08	9.8	2334	2193	0.051	8.2
	F	Mean	410	2.90	95.0	23402	22416	0.537	46.9
		SD	59	7.42	52.1	3676	1403	0.034	7.4

Abbreviations: AUC_{0-480} = area under the curve from 0 to 480 hours, $AUC_{0-\infty}$ = area under the curve from time of dosing extrapolated to infinity, Cl = clearance, C_{max} = concentration corresponding to T_{max}, F = female, M = male, n = number, SD = standard deviation, T_{max} = time of maximum observed concentration, $t_{1/2}$ = terminal half-life, V_z = volume of distribution.

n = 10/sex/group

(Excerpted from Applicant's submission)

Figure 30: Mean (SD) Concentrations of IMC-11F8 (b) (4) in Monkey Serum as a Function of Treatment

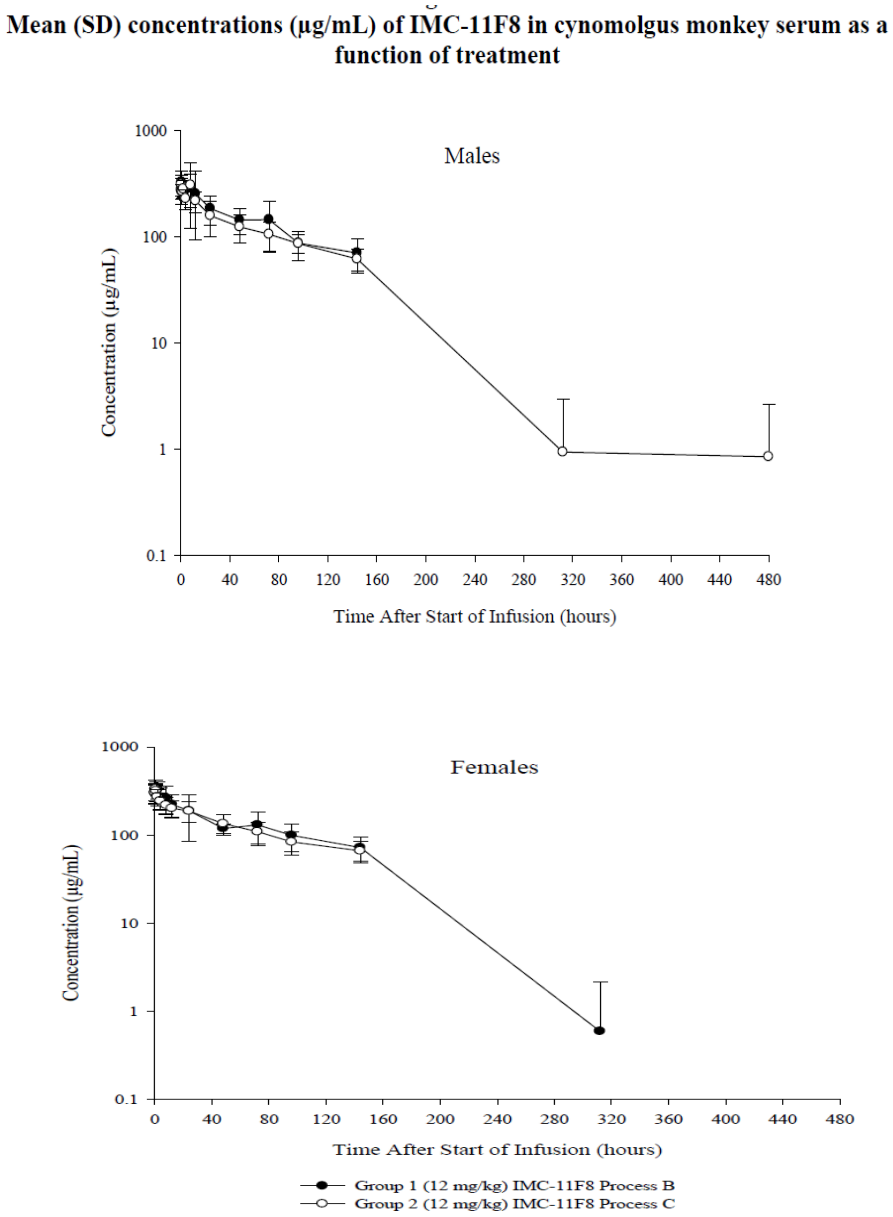

(Excerpted from Applicant's submission)

The Applicant reported that the level of circulating serum IMC-11F8 concentrations in D29 and D38 test samples were ≥ 10 µg/mL, which interfered with the detection of anti-drug antibodies (ADA) capable of binding to IMC-11F8. As a result, most test samples were reported as negative, and immunogenicity study results were difficult to interpret. Six D1 samples, 5 D29 samples, and 7 D38 samples were reported as

ADA-positive; ADA-positive results were approximately equal between [redacted] lots.

The commercial scale process for manufacture of necitumumab drug substance is [redacted] drug product has an active ingredient concentration of 16.0 mg/mL, the same active ingredient concentration as [redacted] Patients administered 800 mg necitumumab in the Phase 2 trial conducted to compare pharmacokinetics between necitumumab drug [redacted] (Study JFCJ) received drug product manufactured using drug substance from both [redacted] (cohort 1) and [redacted] (cohort 2). Pharmacokinetic parameters were similar from both cohorts. The initial commercial product will use [redacted] drug substance.

The Applicant has documented that the primary changes between manufacturing [redacted] include: [redacted]

5.2 Toxicokinetics

Toxicokinetics are included in toxicology studies.

6 General Toxicology

6.1 Single-Dose Toxicity

None

6.2 Repeat-Dose Toxicity

Study title: 5-week repeat-dose study in monkeys with a 6-week recovery phase (Study no. CR0878)

Cynomolgus monkeys were administered necitumumab at 4, 12 and 40 mg/kg weekly on D 1, 15, 22 and 29. Toxicokinetics indicated that drug exposure increased in a greater than proportional manner across doses tested. Immunogenicity analyses were not evaluable. There were no significant drug-related findings. The NOAEL was 40 mg/kg, the highest dose tested.

Study title: A 26-week toxicity, toxicokinetic, and immunogenicity study of IMC-11F8 administered intravenously weekly to cynomolgus monkeys with an 8-week recovery period [Final report amendment No. 1 for this study included a supplemental pathology report – see histopathology section of this study review]

Study no.:	[redacted]. 023.07
Study report location:	M4.2.3.2.2
Conducting laboratory and location:	[redacted]

Date of study initiation:	May 17, 2006
GLP compliance:	Yes (Toxicokinetic analyses were not conducted in compliance with GLP)
QA statement:	Yes
Drug, lot #, and % purity:	IMC-11F8, lot # 2158-30, purity 99% (Note: Manufacturing process of this lot is noted [redacted] (b) (4) in Product Quality data. Certificate of Analysis does not identify manufacturing process or active ingredient (a.i.) concentration. [redacted] (b) (4) lot with a.i. concentration of 16.0 mg/mL will be used commercially.

Key Study Findings

● Single drug-related lethality at HD following ~17 weeks of dosing with injection site hemorrhage and hemorrhage of heart and lung possibly a result of coagulopathy related to sepsis.
● The primary targets were the skin and injection site. Hyperplastic dermatitis, characterized by epidermal hyperplasia, hyperkeratosis, and inflammatory infiltration was observed grossly and microscopically in skin of the abdomen, inguinal area, and ears /nose/mouth, and to a lesser extent in skin of the mammary glands. Findings were observed at all dose levels with a higher incidence in MD and HD animals.
● Diffuse inflammatory infiltration and mineralization was observed in multiple organs and tissues following dosing and recovery in all dose groups.
● Magnesium levels were marginally depressed in males and depressed in females at the MD and HD.
● Degeneration of renal tubular epithelium as observed with cetuximab
● TK indicated that necitumumab exposure was generally dose proportional to greater than dose-proportional. Half-life increased with dose, and clearance following dose 26 decreased ~76% compared to clearance following dose 1. Drug accumulation appeared to increase over time at all doses.

Methods

Doses:	6, 19, and 60 mg/kg (Dose concentrations: 1.2, 3.8 and 12 mg/mL)
Frequency of dosing:	Weekly for 26 weeks
Route of administration:	Intravenous (1 mL/min) via syringe pump to cephalic or saphenous vein ➢ Injection sites marked following each injection ➢ Range of infusion duration during study: 8-15m
Dose volume:	5 mL/kg
Formulation/Vehicle:	[redacted] (b) (4) 40 mM NaCl, [redacted] (b) (4) mannitol, 133 mM glycine, 0.01% Tween 80, pH 6.0
Species/Strain:	Cynomolgus monkey
Number/Sex/Group:	See table below

Age: 3-5 years
Weight: M: 2.8-4.7 kg; F: 2.4-3.7 kg
Satellite groups: None
Unique study design: Toxicokinetic and immunogenicity evaluations conducted on dosed monkeys from each group (see timing of evaluations below)
Deviation from study protocol: These deviations did not impact the overall reliability of the data.

- A report amendment was submitted (Final Report Amendment 1) as a supplemental pathology report to provide additional morphometric analysis of sebaceous glands (including sebocytes) of skin tissue; supplemental dermal observations discussed below
- Palliative treatment (Nolvasan solution, neomycin, polymixin ointment, Humilac) administered for erythemia and dry skin as needed.
- Various clinical observations not conducted or recorded on specific animals throughout the study
- Food consumption data misrecorded or not documented throughout the study
- Thymus/parathyroids, cerebellum, pituitary or mesenteric lymph nodes missing from animals (1 monkey per tissue)
- No hematology slides evaluated for blood cell morphology

Dose group (mg/kg)	Number and designation of animals[a]	
	Males	Females
0	5	5
6	5	5
19	5	5
60	6	6

[a] Three monkeys/sex/group scheduled to be sacrificed on D183 following dosing; two monkeys/sex/group scheduled to be sacrificed on D239 following recovery (Recovery D56)

Observation	Time of Assessment
Mortality	? 2x/day
Clinical observations	2x/day
Dermal observations supplemental to protocol	Weekly by 2 independent observation teams beginning D31 through end of dosing/recovery (see description and exceptions to dermal scoring assessment)
Body weights	Prior to dosing, weekly thereafter, day of necropsy
Food consumption	2x/day (estimates)
Electrocardiography	Prior to dosing, D2, 84, 86, 175, 177 and 237
Hematology	Prior to dosing, D28, 91, 127, and on day prior

	to necropsy (D182 or 238)
Coagulation	Prior to dosing, D28, 91, 127, and on day prior to necropsy (D182 or 238)
Clinical chemistry	Prior to dosing, D28, 91, 127, and on day prior to necropsy (D182 or 238)
Urinalysis	Prior to dosing, D28, 91, 182, 238
Flow cytometry of peripheral blood	Prior to dosing, D91, day prior to necropsy
Toxicokinetics	♦ Full profile: D1, 176 at pre-dose, 10', 1, 3, 6, 12, 24, 72, 120, 168h post-dose ♦ Trough and peak: D29, 57, 92, 120, 148 at pre-dose, 10' post dose ♦ D238 concurrent with immunogenicity sampling
Immunogenicity evaluation	Prior to dosing on D1, 29, 176, 238
Antibody evaluation	Prior to terminal and recovery necropsy (not submitted with study report)
Gross pathology	D183 (terminal sacrifice), D239 (recovery necropsy)
Organ weights	D183 (terminal sacrifice), D239 (recovery necropsy) adrenals, brain, heart, liver, kidneys, lungs, ovaries, pituitary, spleen, thymus, thyroid, uterus, prostate/seminal vesicles, epididymides, testes, submandibular salivary glands
Histopathology	D183 (terminal sacrifice), D239 (recovery necropsy)

Supplemental dermal observations:
Due to findings during general clinical observations, dermal observations were initiated on D31(Week 4/5) through recovery for surviving animals (D234); findings were used to supplement general clinical observations.
A scoring system for skin coloration, condition, and epilation was conducted following each dose. Observations were conducted by 2 assessment teams to minimize observer bias, one team performed observations on the day following dosing and the second team performed observations 1-3 days later. Total scores were averaged. Observations were continued weekly during recovery.

Exceptions to dermal assessment included:
♦ Observations not conducted Weeks 11 and 33
♦ Single set of observations conducted Weeks 5, 6, 9, 26, 28, 31, 32
♦ Observations performed 4 days apart on Week 13
♦ Observations performed by both teams on same day for Weeks 14, 16, 17, 20, 22 and 23

Parameter	6 mg/kg		19 mg/kg		60 mg/kg	
	M	F	M	F	M	F
Mortality	1[a]					1[a]
Clinical observations	♦ Dose responsive manner at all doses with most severe observations at HD: Erythema, dry skin, scaling of skin,					

Parameter	6 mg/kg		19 mg/kg		60 mg/kg	
	M	F	M	F	M	F
	scratching, hunched posture (from D15 – end of dosing) ♦ Erythema noted primarily in inguinal and auxiliary body areas ♦ Dry skin observed over full body ♦ HD administered palliative treatments (Chlorhexidine + bacitracin/neomycin ointment) on severe areas of erythema + Humilac to alleviate discomfort and prevent infection due to scratching ♦ Alopecia, sporadic emesis, soft stool					
Dermal observations supplemental to protocol	See tables and description below					
Body weights[b] Dosing D56-175						↓15-19
Food consumption[b]	UR					
Electrocardiography/BP[b]	UR					
Ophthalmology	UR					
Hematology[b] Platelets[d] (D91/182)	↑11/↑3	↑11/-	↑24/↑22	↑6/↑16	↑47/↑38	↑26/↑36
Coagulation[b] Fibrinogen (D91/182)[e]	- /↑7		↑10/↑24		↑31/↑49	-/↑41
Clinical chemistry[b,f] ALT (D91/182) AST (D91/182) GGT (D91/182) Magnesium (D91/182) Potassium (D91/182)	 ↑74/↑94 ↑32/↑31 ↑9/↑20 ↓7/-	 ↑65/↑35 ↑21/↑38 ↑43/↑79	 ↑71/↑35 ↑59/- ↓7/-	 ↑32/↑11 ↑23/- ↑18/↑44 ↓7/↓7 ↓11/-	 ↑24/↑35 ↑49/- -/↑22 ↓7/↓16 ↓6/-	 - ↑15/- ↑69/↑188 ↓7/↓16 ↓6/-
Urinalysis[b]	UR (Note sample contamination across all groups)					
Flow cytometry of peripheral blood[b]	There were no treatment-related changes in peripheral blood B (CD3-CD20+), or T (CD3+) cells, and no changes in T cell subsets (CD3+CD4+ or CD3+CD8+) or NK cell subsets (CD3-CD16+).					
Toxicokinetics	See below					
Immunogenicity evaluation	See below – Meaningful data interpretation could not be completed					
Gross pathology	Skin lesions at all doses including erythema, scaliness and red to brown crusts overlying erythematous skin. Lesions observed at multiple sites on body including face, arm, inguinal area, abdomen and leg.					
Organ weights (absolute)[b] Kidneys Thymus Prostate/seminal vesicles Testes	 ↑72 ↓47 ↓42	 ↑39	 ↑40 ↓22	 ↑32	 ↑36 ↑1.7 fold ↓56 ↓32	 ↑41
Histopathology	See histopathology table below – Adequate battery conducted					

[a] LDM found dead on D4; death was not drug related – necropsy indicated hemorrhage and rupture in stomach wall caused by pre-existing ulcer.
HDF sacrificed moribund D120 –clinical observations included lethargy, hypothermia, shallow respiration, weakness and recumbency. Bleeding and hematomas were noted at blood draw and dose administration sites. Histopathology noted perivascular hemorrhage at the injection site with additional hemorrhage of heart and lung. The Applicant has indicated that this is not a drug-related death citing coagulopathy related to septicemia, although this reviewer considers the injection site hemorrhage and subsequent need for moribund sacrifice to be consistent with the pharmacology of the biologic. Deaths due to sepsis were also observed in monkeys administered cetuximab following 13 weeks of dosing at the HD.

[b] Percent compared to concurrent control
[c] Blank spaces = no findings or unremarkable results
[d] The dose related increase in platelet count was likely a result of the dermal inflammation observed in these animals. White cell counts were unremarkable.
[e]The dose related increase in fibrinogen may also be a result of the dermal inflammation observed in these animals.
[f] Increased **ALT** and **AST** levels were inversely dose related; increased GGT values inconsistent between gender. Notable that changes were observed towards the end of the dosing period and indices were generally similar to concurrent controls following recovery.
Magnesium levels were marginally depressed in males and depressed in females at the MD and HD. This finding is consistent with hypomagnesemia observed in the clinic. Note that magnesium levels in monkeys remained depressed following recovery.
Potassium levels were depressed in females only

Immunogenicity:

An electrochemiluminescence assay (ECLA) was used to detect anti-IMC-11F8 mAbs following incubation of samples with biotinylated-IMC-11F8 and ruthenylated-IMC-11F8. The assay cutpoint was defined as a signal-to-noise ratio of 1.11. Samples with IMC-11F8 levels above the cut-point were evaluated by a second specificity assay, although antibody detection was limited by serum concentrations of IMC-11F8 equal to or greater than 20 µg/mL which may have interfered with detection of antibodies capable of binding to IMC-11F8 in the assay.

Samples collected on D29 and D179 from animals at all dose groups were negative for anti-drug antibody formation. Following recovery, samples taken on D238 were also negative for LD animals; a single MD and HD animal exhibited measurable antibody following recovery. (The Applicant notes that serum from the HDF sacrificed moribund on D120 exhibited detectable anti-ADA pre-study as well as D120, but was below detectable limits on D29.)

High levels of circulating drug may have saturated the anti-drug-antibody leaving an insufficient quantity of free binding sites for the assay to detect a response. Alternatively, mishandling of samples, non-specification of assay, or failure of assay validation may also have contributed to the difficulty of data interpretation. Three vehicle control animals exhibited positive specificity assay results, and 1 MD and 2 HD animals exhibited positive assay results prior to dosing on D1. The Applicant suggested that serum components from these animals contributed to non-specific binding resulting in a positive assay result. The Applicant also documented that a separate antibody evaluation was conducted prior to terminal and recovery necropsy. These data were not submitted with the study report. When results of antibody evaluation were requested, the Applicant indicated that serum samples had been discarded.

Histopathology:

Histopathological findings of skin lesions were associated with epidermal hyperplasia, hyperkeratosis, lymphocytic inflammation and mononuclear cell infiltrate at the injection site as well as abdominal, ear, inguinal, and mammary dermal sites. These dermal findings are consistent with findings observed with other EGFR-inhibitors.

Histopathology (Terminal necropsy: N = 3/sex/dose; Recovery necropsy: N= 2/sex/dose with exception of HD where N = 3)

Organ/finding	Males (mg/kg)				Females (mg/kg)			
	0	6	19	60	0	6	19	60
Adrenal: hyperplasia, infiltrate, VS		2R		1				
Bone (sternum): hypocellularity, VS								1
Esophagus: infiltrate, mononuclear, VS	1+1R	1+2R	2	1+1R		1	2+1R	2+1R
Heart: infiltrate, mononuclear,VS	1+1R	2R		3+1R		2R	2R	1R
--degeneration, myocardial, VS				1R				
Injection site: hyperkeratosis, S		1		1R		1		
--hyperplasia, VS		1		2		2		1
--infiltrate, mononuclear, VS - S	2	2+1R	2+1R	3+1R		2	1+2R	3
--inflammation, lymphocytic, VS - S			1	2		1		2
--inflammation, subacute/chronic, VS - Mod					2	3	2	1
--hemorrhage, VS - M			1R		1	2	2	1
--sarcosporidiosis, VS							1	1
Kidney: infiltrate, mononuclear, VS	1+1R	2	1R	2+3R	1R	1	2+2R	1+2R
--mineralization, VS	1R	1+1R	3	1+2R	1	3	2	2
--syncytial cells, VS - S	1	1		2	1		2	
--degeneration, VS - S	1		2	1	1	1	1	2+1R
--tubular protein, VS				1R				2+1R
--edema, VS								1
--fibrosis, S								1R
--glomerulosclerosis, VS								1R
Lacrimal gland: infiltrate, mononuclear, VS						1R	1R	1R
Epididymides: absence of spermatozoa*		1		1				
Liver: infiltrate, mononuclear, VS	1R	2+1R	1+1R	2+2R				
--fibrosis, VS		1						
--brown pigment deposition, VS - Mod						2		
--hyperplasia, VS - S		2R				2		
Large intestine (cecum): hyperplasia, VS - M					1	2		1+1R
--inflammation, Mod						1		
Lung: aggregation/macrophages, VS				1		1		1
-- infiltrate, mononuclear, VS		1	1	1+2R				
--pigment, anthraco-silicotic	2R	2R	2R	3R	2R	2R	2R	2R
Lymph node, mandibular: hyperplasia VS	1			2+1R				
--erythrosis, erythrophagocytosis, VS				1R				
Lymph node, mesenteric: hyperplasia VS				1		1		
--increased macrophage VS				1				
--pigmented macrophage, VS							1R	1R
Mammary: hyperplasia, VS						1		1
--infiltrate, neutrophilic, VS - S				2R		2		2

Organ/finding	Males (mg/kg)				Females (mg/kg)			
	0	6	19	60	0	6	19	60
Ovaries: mineralization, multifocal, VS						1+2R	1R	1
--follicle reduction, S							1	
Prostate: infiltrate, mononuclear, VS	1R	1R	2+1R					
Skin, abdominal: hyperkeratosis VS - S				1		2		1
--hyperplasia VS - S		1	1	3+1R		3	3	2+2R
--infiltrate, mononuclear, VS - S	2	2	3+1R	3+2R	1	3	3+1R	2+2R
--inflammation, VS			1	1		2	2	1R
Skin, ear: infiltrate, mononuclear, VS		1	1+1R	1		2	1R	1+2R
--infiltrate, neutrophilic, VS						1		1
--inflammation, VS								1+2R
--hyperkeratosis, VS - S			1R	2R		1		3
--hyperplasia, VS			2R	2R				1+2R
Skin, inguinal: hemorrhage, VS - S		1	1			1	1	1
--hyperkeratosis, VS - Mod				2				2
--hyperplasia VS - Mod			2+1R	3+1R		1	2	3+2R
--infiltrate, mononuclear, VS		1	1+1R	3+2R		2	2	3
--inflammation, VS - Mod			1	2				1+2R
Skin, mammary: hyperplasia, VS - S		1		2		2		1
-- infiltrate, mononuclear, VS		1	1	2		3+1R		1
--inflammation				1			1	1
--hyperkeratosis, VS - S						1		1
Skin, composite/all sites/gross lesions: hyperkeratosis, VS - Mod		1	2	2		2		3
--hyperplasia, VS - Mod		2	2	3		3	3	3
--inflammation, VS - Mod		1	2	3		2	2	2
Small intestine: hyperplasia, VS				1R		1	1	
Spleen: brown pigment, Mod						1		
Submandibular gland: infiltrate, mononuclear, VS*	2	1	1	2	1	2	1	2
Testes: immature, degeneration, VS	2R	1+2R	1+2R	2+3R				
--dilatation/seminiferous tubules, VS - S		2	1	1				
Thymus:involution, VS - S		2R	1R	1R				
Urinary bladder: infiltrate, mononuclear, VS								1R

Abbreviations: VS = very slight; S = slight; * = finding not graded; Mod = moderate; M = marked
Note: Finding not documented if incidence in controls = incidence in treated animals

Note: Histopathological findings in the female decedent included but not limited to marked hemorrhage + slight hyperkeratosis, hyperplasia, and mononuclear cell infiltrate of the injection site; moderate edema + slight hemorrhage of the lung, and slight acute hemorrhage of the heart. The Applicant considers these findings to be suggestive of terminal coagulopathy.

A supplemental morphometric examination of skin tissue histopathology (Amendment No. 1) was conducted to analyze sebaceous glands and sebocytes. Results indicated that significant differences in the sebaceous gland area was observed in the abdominal and ear skin of LD males when compared with concurrent controls; these differences were not observed in MD or HD males or any dosed female group when compared to controls. The Applicant did not consider these differences to be drug-related.

Table 4: Dermal observation scoring system

Score	Coloration	Condition	Epilation
1	Normal	Normal	None
2	Pale pink	Petechiation/ Erythema	Mild, patchy
3	Pink	Discharge	Mild-moderate, patchy to diffuse
4	Bright pink	Skin breaks	Moderate, diffuse
5	Pink-red	Erosions	Moderate-severe, diffuse
6	Red		Severe

According to the scoring system noted above, the following tables summarize the dermal observations over the dosing period and were excerpted from the Applicant's submission.

Skin coloration, condition and epilation were elevated in a dose-related manner beginning on W5 and continuing through W26. The most severe findings were observed at the HD; there were generally no gender differences. Findings in LD and MD monkeys appeared to resolve to a greater degree following recovery. Palliative treatment was administered to HD monkeys as needed.

Table 5: Dermal observation results following dosing of IMC-11F8

Notes: SSAN = animal number; NA = Not available; SSAN #37 was found moribund and sacrificed (HDF noted above).

Group No./ Dose	SSAN	SEX	Study Week 5	Study Week 6	Study Week 7	Study Week 8	Study Week 9	Study Week 10	Study Week 11	Study Week 12	Study Week 13	Study Week 14	Study Week 15	Study Week 16
1 Vehicle (0 mg/kg)	1	F	1.0	1.0	1.0	1.0	1.0	1.0	NA	1.0	1.0	1.0	1.0	1.0
	2	M	1.0	1.0	1.0	1.0	1.0	1.0	NA	1.0	1.0	1.0	1.0	1.0
	3	F	1.0	1.0	1.0	1.0	1.0	1.0	NA	1.0	1.0	1.0	1.0	1.0
	4	M	1.0	1.0	1.0	1.0	1.0	1.0	NA	1.0	1.0	1.0	1.0	1.0
	5	F	1.0	1.0	1.0	1.0	1.0	1.0	NA	1.0	1.0	1.0	1.0	1.0
	6	M	1.0	1.0	1.0	1.0	1.0	1.0	NA	1.0	1.0	1.0	1.0	1.0
	7	F	1.0	1.0	1.0	1.0	1.0	1.0	NA	1.0	1.0	1.0	1.0	1.0
	8	M	1.0	1.0	1.0	1.0	1.0	1.0	NA	1.0	1.0	1.0	1.0	1.0
	9	F	1.0	1.0	1.0	1.0	1.0	1.5	NA	1.5	1.5	1.5	1.5	1.5
	10	M	1.0	1.0	1.0	1.0	1.0	1.0	NA	1.0	1.0	1.0	1.0	1.0
		Mean	1.0	1.0	1.0	1.0	1.0	1.1		1.1	1.1	1.1	1.1	1.1
		SD	0.0	0.0	0.0	0.0	0.0	0.2		0.2	0.2	0.2	0.2	0.2
2 IMC-11F8 (6 mg/kg)	11	F	1.0	1.0	1.5	1.0	1.0	1.0	NA	1.0	1.0	1.0	1.0	1.0
	12	M	1.0	1.0	1.0	1.0	1.0	1.0	NA	1.0	1.0	1.0	1.0	1.0
	13	F	2.0	2.0	2.0	2.0	2.0	1.5	NA	2.0	1.0	1.0	1.5	1.5
	14	M	1.0	1.0	1.0	1.0	1.0	1.0	NA	1.0	1.0	1.0	1.0	1.0
	15	F	1.0	1.0	1.0	1.0	1.0	1.5	NA	1.0	1.0	1.0	1.5	1.0
	16	M	1.0	2.0	1.0	1.0	1.0	1.0	NA	1.0	1.0	1.5	1.0	1.0
	17	F	2.0	2.0	2.5	1.5	3.5	2.0	NA	1.0	1.0	1.0	1.5	1.5
	18	M	1.0	2.0	1.0	1.0	1.0	1.0	NA	1.0	1.0	1.0	1.0	1.0
	45	F	1.0	1.0	1.0	2.0	1.0	NA	1.5	1.5	1.5	1.5	1.5	1.5
	20	M	1.0	1.0	1.0	2.5	1.0	1.0	NA	1.0	1.0	1.0	1.0	1.0
		Mean	1.2	1.4	1.3	1.4	1.4	1.2	1.5	1.2	1.1	1.1	1.2	1.2
		SD	0.4	0.5	0.5	0.6	0.8	0.4		0.3	0.2	0.2	0.3	0.2

Group No./ Dose	SSAN	SEX	Study Week 5	Study Week 6	Study Week 7	Study Week 8	Study Week 9	Study Week 10	Study Week 11	Study Week 12	Study Week 13	Study Week 14	Study Week 15	Study Week 16
3 IMC-11F8 (19 mg/kg)	21	F	2.0	1.0	1.5	1.5	1.0	1.8	NA	1.0	1.0	1.5	1.0	1.0
	22	M	1.0	1.0	1.0	1.0	1.0	1.0	NA	1.0	1.0	1.0	1.0	1.0
	23	F	1.0	1.0	1.0	1.0	1.0	1.0	NA	1.0	1.0	1.0	1.0	1.5
	24	M	1.0	1.0	1.0	1.0	1.0	1.5	NA	1.0	1.0	1.0	1.5	1.5
	25	F	2.0	1.0	2.0	2.0	2.0	1.5	NA	1.0	1.5	1.5	1.5	1.5
	26	M	1.0	1.0	1.0	1.0	1.0	1.0	NA	1.0	1.0	1.0	1.0	1.0
	27	F	1.0	1.0	1.5	1.0	2.0	1.0	NA	1.5	1.0	1.0	1.0	1.0
	28	M	1.0	1.0	1.0	1.0	2.0	1.0	NA	1.0	1.0	1.0	1.0	1.0
	29	F	2.0	2.0	2.0	2.0	1.0	2.0	NA	2.0	1.5	1.5	2.5	2.0
	30	M	1.0	2.0	1.0	1.5	1.0	1.8	NA	1.5	2.0	1.0	1.5	2.0
		Mean	1.3	1.2	1.3	1.3	1.3	1.4		1.2	1.2	1.2	1.3	1.4
		SD	0.5	0.4	0.4	0.4	0.5	0.4		0.3	0.3	0.2	0.5	0.4
4 IMC-11F8 (60 mg/kg)	31	F	1.0	1.0	1.0	1.0	2.0	1.0	NA	1.0	1.0	1.0	1.0	1.0
	32	M	2.0	2.5	3.0	2.8	3.0	3.3	NA	3.0	2.5	2.0	2.5	2.5
	33	F	1.0	1.0	1.0	1.0	1.0	1.5	NA	1.0	1.5	1.0	1.0	1.5
	34	M	1.0	2.0	1.5	1.0	1.0	1.0	NA	1.0	1.5	1.0	1.0	1.0
	35	F	2.0	2.0	1.5	1.5	2.0	1.5	NA	1.5	2.0	1.5	1.0	1.5
	36	M	1.0	1.0	1.0	1.0	1.0	1.0	NA	1.0	1.0	1.0	1.5	1.0
	37**	F	1.0	1.0	1.5	2.0	1.0	1.0	NA	1.0	2.0	1.0	1.0	1.5
	38	M	1.0	2.0	2.0	2.0	2.0	1.5	NA	1.0	1.5	1.5	1.5	1.5
	39	F	3.0	5.0	4.0	3.8	3.0	4.3	NA	3.5	4.0	4.5	5.0	4.3
	40	M	2.0	2.0	1.5	1.5	3.0	2.5	NA	1.0	2.0	1.5	1.5	1.0
	41	F	2.0	1.0	1.5	2.3	1.0	3.0	NA	3.0	3.0	4.0	3.5	3.8
	42	M	1.0	1.0	1.0	2.0	1.0	1.5	NA	1.0	1.5	1.5	1.0	1.0
		Mean	1.5	1.8	1.7	1.8	1.8	1.9		1.6	2.0	1.8	1.8	1.8
		SD	0.7	1.2	0.9	0.8	0.9	1.1		1.0	0.9	1.2	1.3	1.1

Group No./ Dose	SSAN	SEX	Study Week 17	Study Week 18	Study Week 19	Study Week 20	Study Week 21	Study Week 22	Study Week 23	Study Week 24	Study Week 25	Study Week 26	Study Week 27
1 Vehicle (0 mg/kg)	1	F	1.0	1.0	1.0	1.0	1.0	1.0	1.0	1.0	1.0	1.0	NA
	2	M	1.0	1.0	1.0	1.0	1.0	1.0	1.0	1.0	1.0	1.0	NA
	3	F	1.0	1.0	1.0	1.0	1.0	1.0	1.0	1.0	1.0	1.0	NA
	4	M	1.0	1.0	1.0	1.0	1.0	1.0	1.0	1.0	1.0	1.0	NA
	5	F	1.0	1.0	1.0	1.0	1.0	1.0	1.0	1.0	1.0	1.0	NA
	6	M	1.0	1.0	1.0	1.0	1.0	1.0	1.0	1.0	1.0	1.0	NA
	7	F	1.0	1.0	1.0	1.0	1.0	1.0	1.0	1.0	1.0	1.0	1.0
	8	M	1.0	1.0	1.0	1.0	1.0	1.0	1.0	1.0	1.0	1.0	1.0
	9	F	1.5	1.0	1.5	1.5	1.5	1.0	1.3	1.5	1.3	1.0	1.0
	10	M	1.0	1.0	1.0	1.0	1.0	1.0	1.0	1.0	1.0	1.0	1.0
		Mean	1.1	1.0	1.1	1.1	1.1	1.0	1.0	1.1	1.0	1.0	1.0
		SD	0.2	0.0	0.2	0.2	0.2	0.0	0.1	0.2	0.1	0.0	0.0
2 IMC-11F8 (6 mg/kg)	11	F	1.0	1.0	1.0	1.0	1.0	1.0	1.0	1.5	1.0	2.0	NA
	12	M	1.0	1.0	1.0	1.0	1.0	1.0	1.0	1.0	1.0	1.0	NA
	13	F	2.0	2.0	2.0	2.0	1.0	1.0	2.0	2.0	1.5	1.0	NA
	14	M	1.0	1.0	1.0	1.0	1.0	1.0	1.0	1.0	1.0	1.0	NA
	15	F	1.0	1.5	1.0	1.0	1.0	1.0	2.0	1.5	1.0	1.0	1.5
	16	M	1.0	1.5	1.0	1.0	1.0	1.0	1.0	1.5	1.0	1.0	NA
	17	F	1.0	2.5	1.0	2.0	1.5	1.5	1.5	1.5	1.5	1.0	2.0
	18	M	1.0	1.0	1.0	1.0	1.0	1.0	1.0	1.0	1.0	1.0	1.0
	45	F	1.0	1.5	1.5	1.5	1.5	1.0	1.5	1.5	1.0	1.0	NA
	20	M	1.0	1.0	1.0	1.0	1.0	1.0	1.0	1.0	1.0	1.0	1.0
		Mean	1.1	1.4	1.2	1.3	1.1	1.1	1.3	1.4	1.1	1.1	1.4
		SD	0.3	0.5	0.3	0.4	0.2	0.2	0.4	0.3	0.2	0.3	0.5

Group No./ Dose	SSAN	SEX	Study Week 17	Study Week 18	Study Week 19	Study Week 20	Study Week 21	Study Week 22	Study Week 23	Study Week 24	Study Week 25	Study Week 26	Study Week 27
3 IMC-11F8 (19 mg/kg)	21	F	1.0	1.5	1.0	1.5	2.0	1.5	1.5	2.0	1.0	1.0	NA
	22	M	1.0	1.0	1.0	1.0	1.0	1.0	1.0	1.0	1.0	1.0	NA
	23	F	1.5	1.0	1.0	1.0	1.0	1.0	1.0	1.0	1.0	1.0	NA
	24	M	1.0	1.5	1.5	2.0	1.5	1.5	1.8	1.5	2.0	1.0	NA
	25	F	2.0	1.5	1.0	1.5	1.5	1.5	1.8	2.0	1.5	2.0	NA
	26	M	1.0	1.0	1.0	1.0	1.0	1.0	1.0	1.0	1.0	1.0	NA
	27	F	1.0	1.5	1.0	2.5	1.0	1.0	1.5	1.0	1.5	1.0	1.5
	28	M	1.0	1.0	1.0	1.0	1.0	1.0	1.0	1.0	1.5	1.0	1.5
	29	F	2.5	2.5	1.5	2.0	2.0	1.5	2.0	1.5	2.5	2.0	1.0
	30	M	2.0	2.5	1.0	2.0	1.5	1.5	2.0	2.0	1.0	2.0	1.0
		Mean	1.4	1.5	1.1	1.6	1.4	1.3	1.5	1.4	1.4	1.3	1.3
		SD	0.6	0.6	0.2	0.6	0.4	0.3	0.4	0.5	0.5	0.5	0.3
4 IMC-11F8 (60 mg/kg)	31	F	1.0	1.5	1.0	1.0	3.5	3.5	3.8	4.5	3.5	3.0	3.5
	32	M	2.5	3.5	2.5	2.8	2.5	2.5	2.5	2.5	4.5	3.0	NA
	33	F	1.5	2.5	1.5	1.0	1.5	1.0	1.5	1.0	1.5	2.0	NA
	34	M	1.0	2.0	1.0	1.0	1.0	1.0	1.0	1.0	1.0	1.0	NA
	35	F	2.0	1.5	2.0	1.5	2.0	2.0	2.0	2.0	2.0	2.0	NA
	36	M	1.0	1.5	1.0	1.0	1.0	1.0	1.0	1.5	1.5	2.0	NA
	37**	F	1.0	NA	NA	NA	NA	NA	NA	NA	NA	NA	NA
	38	M	2.0	2.5	1.5	1.5	1.5	1.5	1.0	2.0	1.5	2.0	1.5
	39	F	4.0	5.0	5.0	4.8	4.5	4.5	4.5	5.0	5.5	4.0	NA
	40	M	1.5	2.5	2.0	2.5	2.0	2.0	2.3	2.0	2.0	3.0	1.5
	41	F	3.0	4.5	4.0	4.5	3.8	4.5	4.5	4.5	5.0	5.0	3.5
	42	M	1.0	2.0	1.0	1.0	1.0	1.5	2.0	1.5	2.0	2.0	1.0
		Mean	1.8	2.6	2.0	2.0	2.2	2.3	2.4	2.5	2.7	2.6	2.2
		SD	1.0	1.2	1.3	1.4	1.2	1.3	1.3	1.5	1.6	1.1	1.2

Group No./ Dose	SSAN	SEX	Study Week 28	Study Week 29	Study Week 30	Study Week 31	Study Week 32	Study Week 34
1 Vehicle (0 mg/kg)	1	F	NA	NA	NA	NA	NA	NA
	2	M	NA	NA	NA	NA	NA	NA
	3	F	NA	NA	NA	NA	NA	NA
	4	M	NA	NA	NA	NA	NA	NA
	5	F	NA	NA	NA	NA	NA	NA
	6	M	NA	NA	NA	NA	NA	NA
	7	F	1.0	1.0	1.0	1.0	1.0	1.0
	8	M	1.0	1.0	1.0	1.0	1.0	1.0
	9	F	1.0	1.0	1.0	1.0	1.0	1.0
	10	M	1.0	1.0	1.0	1.0	1.0	1.0
		Mean	1.0	1.0	1.0	1.0	1.0	1.0
		SD	0.0	0.0	0.0	0.0	0.0	0.0
2 IMC-11F8 (6 mg/kg)	11	F	NA	NA	NA	NA	NA	NA
	12	M	NA	NA	NA	NA	NA	NA
	13	F	NA	NA	NA	NA	NA	NA
	14	M	NA	NA	NA	NA	NA	NA
	15	F	2.0	1.5	1.0	2.0	3.0	1.5
	16	M	NA	NA	NA	NA	NA	NA
	17	F	1.0	1.5	1.0	2.0	2.5	1.5
	18	M	1.0	1.0	1.0	1.0	1.0	1.0
	45	F	NA	NA	NA	NA	NA	NA
	20	M	1.0	1.0	1.0	1.0	1.0	1.0
		Mean	1.3	1.3	1.0	1.5	1.9	1.3
		SD	0.5	0.3	0.0	0.6	1.0	0.3

Group No./ Dose	SSAN	SEX	Study Week 28	Study Week 29	Study Week 30	Study Week 31	Study Week 32	Study Week 34
3 IMC-11F8 (19 mg/kg)	21	F	NA	NA	NA	NA	NA	NA
	22	M	NA	NA	NA	NA	NA	NA
	23	F	NA	NA	NA	NA	NA	NA
	24	M	NA	NA	NA	NA	NA	NA
	25	F	NA	NA	NA	NA	NA	NA
	26	M	NA	NA	NA	NA	NA	NA
	27	F	1.0	1.0	1.0	1.0	1.0	1.0
	28	M	1.0	1.0	1.0	1.0	1.0	1.0
	29	F	2.0	1.5	2.0	2.0	2.0	2.0
	30	M	1.0	1.0	1.0	2.0	2.0	1.5
		Mean	1.3	1.1	1.3	1.5	1.5	1.4
		SD	0.5	0.3	0.5	0.6	0.6	0.5
4 IMC-11F8 (60 mg/kg)	31	F	3.5	4.0	3.5	2.0	2.0	1.0
	32	M	NA	NA	NA	NA	NA	NA
	33	F	NA	NA	NA	NA	NA	NA
	34	M	NA	NA	NA	NA	NA	NA
	35	F	NA	NA	NA	NA	NA	NA
	36	M	NA	NA	NA	NA	NA	NA
	37**	F	NA	NA	NA	NA	NA	NA
	38	M	1.0	1.0	2.0	1.0	1.0	1.0
	39	F	NA	NA	NA	NA	NA	NA
	40	M	1.0	1.5	1.5	1.0	1.0	1.5
	41	F	4.0	3.5	3.5	5.0	4.0	3.3
	42	M	1.0	2.0	2.0	1.0	1.0	1.0
		Mean	2.1	2.4	2.5	2.0	1.8	1.6
		SD	1.5	1.3	0.9	1.7	1.3	1.0

(Excerpted from Applicant's submission)

Toxicokinetics

Serum levels of IMC-11F8 were assessed using an ELISA-based antigen capture technique (soluble EGF extracellular domain [sEGF/ECD]). Following incubation in sEGF/ECD coated wells, IMC-11F8 was detected with a human kappa IgG1 antibody conjugated to horseradish peroxidase. The LLOQ for the assay was 1 µg/mL. Exposure increase was generally greater than proportional with dose following Doses 1 and 26 (first and last doses, respectively). Half-life increased with dose. Clearance following dose 26 decreased ~76% compared to clearance following dose 1. Drug accumulation appeared to increase over time at all doses. See table and figure excerpted from Applicant's submission below. Drug levels in males were generally elevated compared

to females following each infusion period, although pre-infusion trough levels were similar between genders.

Table 6: Mean toxicokinetic parameters following dosing of IMC-11F8

PK Parameter	Dose 1			Dose 26		
Dose (mg/kg)	**6**	**19**	**60**	**6**	**19**	**60**
C_{max} (µg/mL)	156	585	1979	267	626	2826
C_{min} [a] (µg/mL)	20	122	556	72	238	959
$t_{½}$ (hour)	88	139	263	179	145	222
$AUC_{(0-\infty)}$ (h·µg/mL)	11240	60629	333092	45707	101994	524533
Cl (mL/h/kg)	0.581	0.333	0.282	0.238	0.228	0.138
Vss (mL/kg)	66	57	57	38	41	36

a - C_{min} observed at 168 hours following infusion

Figure 31: Mean IMC-11F8 peak and trough serum concentrations vs time (h)/dose

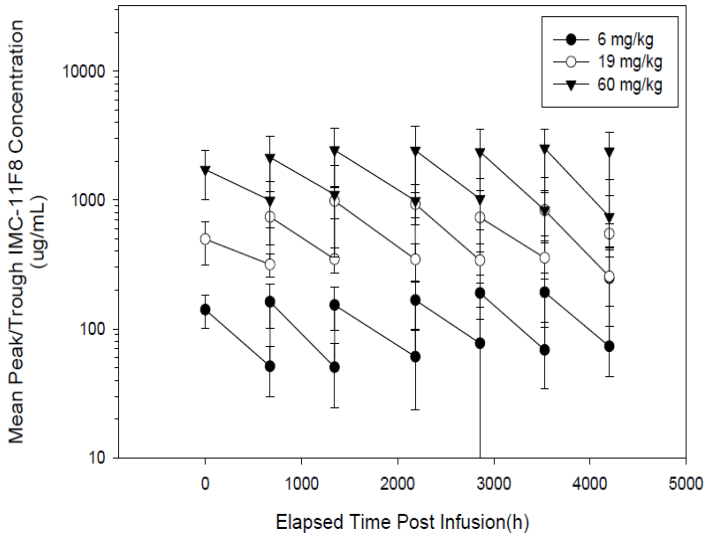

7 Genetic Toxicology

Not conducted and not warranted for an antibody

8 Carcinogenicity

Not conducted and not warranted for an product intended for the treatment of advanced cancer.

9 Reproductive and Developmental Toxicology

Reproductive toxicity studies, including embryofetal development studies, with necitumumab were not conducted. Instead, the Applicant conducted a literature based assessment of the potential for necitumumab to cause developmental toxicity. Some of the key points of supporting the potential developmental effects of EGFR signaling disruption are discussed in this review.

In mice, maternal levels of circulating EGF correlate with fetal growth. When sialoadenctomy was performed on Day 13 (E13) of pregnancy in mice, EGF levels in dams were decreased. This decrease resulted in reduced fetal weight in this model though fetal brain and placental weights were unaffected. When dams received exogenous EGF, fetal weight was comparable to fetal weights observed from control, non-sialoadenectomized, dams (Kamei et al., 1999)[3]. The developmental data from EGF depletion studies suggest an important role for EGF/EGFR signaling in fetal growth.

To directly examine the physiological role of the epidermal growth factor receptor during development, Sibilia and Wagner (1995)[4] generated mice that lacked EGFR by disrupting part of the first exon of the *EGFR* gene with a lacZ reporter gene The resultant animals showed different degrees of disruption in epithelial proliferation and differentiation based on their genetic background. Retardation in growth and death during mid-gestation occurred in mice on the 129/Sv (129) background, while EGFR-/- mice on a 129 x C57Bl/6 (BL6) background survived until birth and some mice on the 129 x BL6 x MF1 background survived until postnatal day 20. The authors hypothesized that death of embryos in utero probably resulted from a defect in the spongiotrophoblast layer of the placenta. Surviving newborn EGFR knockout mice on the 129 x BL6 background had open eyes, rudimentary whiskers, immature lungs, and defects in the epidermis that correlated with the expression pattern of EGFR.

Miettinen et al (1995)[5] developed EGFR KO mice by inactivating exon 2 rather than exon 1, resulting in mice with a similar phenotype to the Sibilia and Wagner model described above. Limited numbers of Miettinen's homozygotic EGFR-/- mice survived until birth (~13%), with embryonic lethality occurring as early as Embryonic Day 10 (E10). Viable EGFR-/- embryos isolated at E10-17 developed normally, though half of them were smaller in size with proportionally smaller placentas than heterozygous and WT littermates (final weight 2 g compared to 6 g). About one third of the smallest EGFR -/- mice had cleft palates. In this model, all surviving EGFR -/- mice were born with open eyes, had short curly whiskers, and died within 8 days. These mice had rapid heart rates, delayed eyelid development, and a one-day delay in external ear opening. The epidermis of newborn EGFR -/- mice was thinner and contained fewer hair follicles than that of weight-matched littermates or *waived-2* mice ($EGFR^{wa2}$), which have attenuated EGFR signaling due to a mutation in the kinase domain of EGFR.

In a third EGFR knockout (KO) model, embryos had defects in skin, lung, and brain leading to differential lethality, again depending on background strain. Surviving mutant mice developed progressive neurodegeneration in the frontal cortex and olfactory bulb, along with defects in the development of eyes, teeth, kidneys, and lungs (Threadgill et al., 1995)[6]. Additional studies done by Sibilia et al. (1998)[7] to further investigate the progressive neurodegeneration observed in multiple EGFR-/- models where there was postnatal survival showed that EGFR signaling is involved in the proliferation and differentiation of astrocytes and in survival of post mitotic neurons in vivo.

The EGFR -/- mice generated by Threadgill also had an impaired intestinal phenotype, consisting of various degrees of hemorrhagic and distended intestines, fewer intestinal loops, and shorter and fewer villi leading to a deficient digestive capacity in newborn mice that ultimately resulted in death. Some of the EGFR -/- mice had dark-colored intestinal loops, fluid in the abdominal cavity, and a histological phenotype that resembled necrotizing enterocolitis, a human disease associated with premature birth.

The lungs of the Threadgill EGFR -/- mice were condensed, with collapsed alveoli close to the pleural surface, or with dilated terminal bronchi closer to the pleura and the alveolar septae that were thicker compared to those of control mice; severe respiratory distress leading to death shortly after birth occurred in many EGFR -/- pups. Similar observations were noted in the Miettinen EGFR -/- mice.

Based on the presented literature, disruption of EGFR can have clear detrimental effects, including significant effects on placental, lung, skin, cardiac, and neural development which can lead to embryofetal and postnatal death, and clear phenotypic signs of teratogenicity. While the available literature was sufficient to demonstrate a clear requirement for EGFR signaling at multiple points in development, it remained unclear whether blocking EGFR signaling with an antibody would result in similar effects. In addition, a murine reduction of function mutant cited by Applicant, the $EGFR^{wa2}$ mouse, is viable and develops normally, but has wavy hair, impaired lactation, and delayed onset of puberty, abnormal ovulation, enlarged aortic valves and cardiac hypertrophy, decreased body size, and increased susceptibility to colitis[8]. Whether the antibody might have a strong teratogenic effect versus a purely embryolethal effect was, therefore, an outstanding question. In order to investigate the potential effects of incomplete blockade of EGFR signaling with an antibody, the Applicant was able to provide surrogate data by right of reference to the reproductive toxicology study conducted as a post-marketing requirement for the anti-EGFR antibody cetuximab. As discussed in the pharmacology sections of this review, cetuximab and necitumumab bind to the same domain of EGFR with similar affinities and have comparable effects on EGFR ligand binding, downstream signaling, and anti-tumor activities. Both antibodies are also able to mediate ADCC. This comparability suggests that cetuximab is a reasonable surrogate for necitumumab in a non-human primate study being used to support the potential developmental effects of the new antibody in the context of the available data from the literature. Cetuximab was detected in amniotic fluid and the serum of embryos from treated dams and, as suggested by the available data from

knockout animals, caused embryolethality and abortions at clinically relevant doses. Based on the totality of the data, necitumumab has the potential to cause fetal harm when administered to pregnant women.

10 Special Toxicology Studies

Study No. 0409: IHC staining of IMC-11F8 for frozen sections of human, monkey and rat tissues
Study No. IM993: Tissue binding study of Fluorescein-labeled monoclonal antibody IMC-11F8 with normal human and cynomolgus monkey tissues

Tissue cross reactivity studies were conducted to assess the ability of anti-human EGFR antibody IMC-11F8 (FITC-labeled 11F8) to bind frozen human, monkey and rat tissues. In Study 0409, IMC- 11F8 bound to human and monkey EGFR in skin, primarily basal epidermal cells, but not to rat skin.

In study IM993, IMC-11F8 reacted with human and monkey epithelium, endocrine cells, myoepithelium, neural tissues, stromal cells, mononuclear/phagocyte cells, smooth muscle and mesothelium. Many tissues displaying IMC-11F8-specific staining were limited to only cytoplasmic staining due to stain limitations. In addition, the staining of several human tissues was not observed in monkey tissues. These included nerves of heart and striated muscle, uterine epithelium, peripheral nerve Schwann cells, myoepithelium of salivary gland and prostate, and spinal cord.

11 Integrated Summary and Safety Evaluation

Pharmacology

Necitumumab is a fully human anti-EGFR IgG1 monoclonal antibody that blocks interaction between EGFR and its ligands. The Applicant provided data to demonstrate that necitumumab binds strongly to ErbB1 with an EC_{50} of ~15 pM, but not to other members of the EGFR family. As measured by surface plasmon resonance, the binding affinity (Kd) for necitumumab to rhEGFR was approximately 0.32 nM, which is very similar to of the affinity of cetuximab (a chimeric IgG1 mAb) for rhEGFR (0.38 nM). Both cetuximab and necitumumab bind to nearly identical epitopes on domain III of the EGFR molecule, and are hypothesized to inhibit receptor activation by blocking the ligand binding site and sterically inhibiting receptor dimerization (Li *et al*., 2008).

To support the use of the cynomolgus monkey as a relevant toxicology species, the Applicant demonstrated that the necitumumab binds with comparable affinity to EGFR derived from humans and cynomolgus monkeys (EC50s of 6-7 pM), but has much lower affinity for rodent-derived EGFR.

The Applicant demonstrated that binding of necitumumab to EGFR inhibited receptor signaling as indicated by inhibition of EGF binding and reduced phosphorylated EGFR (pEGFR) levels. In a separate study, the Applicant demonstrated that inhibition of EGFR activation, as measured by decreased pEGFR levels, correlated with reduced levels of

activated p44/42 MAPK, downstream signaling targets of EGFR, as well as with reduced colon cancer cell proliferation in culture. The extent of inhibition by necitumumab was nearly identical to that observed with cetuximab in this assay. Using a fusion construct in which EGFR was fused to the green fluorescent protein (GFP), necitumumab binding to EGFR led to receptor internalization, lysosomal translocation and degradation (as evident from the diminution of the GFP signal following internalization).

Necitumumab was tested in a large number of murine xenograft studies, both alone and in combination with other biologics and/or chemotherapy regimens, including the combination of gemctibine and cisplatin used in the clinical trial supporting the efficacy of necitumumab in squamous cell carcinoma. Necitumumab exhibited dose-related anti-tumor activity in a number of models of NSCLC, pancreatic and colorectal cancers. In some of the most sensitive models, suppression of tumor growth could be observed at doses as low as 0.3 mg/kg; however, in numerous other models, incomplete suppression was observed even at doses as high as 60 mg/kg, suggesting that EGFR was not the primary turmorigenic mediator in those systems.

Consistent with the potential for Fc effector function of a glycosylated IgG1 antibody, necitumumab was able to bind CD16a and, like cetuximab, mediate ADCC. The Applicant did not assess the ability of necitumumab to mediate complement-mediated cytolysis (CDC). Aglycosylation is considered a potentially desirable property for the purposes of manufacturing; however, it is often associated with reduced pharmacological activity, particularly for functions that rely on effector activity; thus, the Applicant sought to compare the anti-tumor activity of an aglycosylated form of necitumumab to the glycosylated form to determine whether Fc glycosylation was required to mediate anti-tumor activities in these models. The aglycosylated version of necitumumab inhibited tumor growth of EGFR-expressing cells in mouse xenograft models comparably to the glycosylated forms of the antibody in the models evaluated. The Applicant did not evaluate whether the agly-necitumumab possessed effector functions in these models, and, therefore, could not separate effects potentially mediated by effector functions from those resulting from deprivation of growth-factor signaling.

Pharmacokinetics

Necitumumab manufacturing process lots (b) (4) were compared for bioequivalency using pharmacokinetic parameters and immunogenicity testing in monkeys. Necitumumab (b) (4) have been used for nonclinical and clinical studies. The commercial scale process for manufacture of necitumumab drug substance is (b) (4) drug product has the same active ingredient concentration as (b) (4) Pharmacokinetic parameters including exposure were found to be clinically bioequivalent between the process lots (b) (4)

The Applicant evaluated the in vivo pharmacokinetics of necitumumab following IV administration to cynomolgus monkeys. Necitumumab exposure increased with increasing dose and was generally greater than dose proportional in monkeys treated for 26 weeks. The half-life increased with dose from ~3.5 to 11 days, which compares with a half-life of approximately ~12 days clinically. After 26 weeks of dosing in monkeys, the half-life increased 2-fold at the low dose, but remained similar at the mid- and high doses. Drug accumulation increased over time at all doses Necitumumab levels in male monkeys were generally elevated compared to females, although pre-infusion trough levels were similar between gender. Exposures in the 26-week monkey study (using AUC exposure data from monkeys administered 19 mg/kg) were approximately equal to the clinical AUC of 105,000 ug*hr/mL when necitumumab was administered at a dose of 800 mg on a once weekly for 2 weeks of each 3-week cycle. In the clinical trial used to support drug approval, inter-individual variability in necitumumab pharmacokinetic parameters was moderate to high.

The immunogenicity of necitumumab could not be accurately assessed in animal models. High levels of circulating necitumumab may have saturated the anti-drug antibody leaving an insufficient quantity of free binding sites for the assay to detect a response. In addition, mishandling of samples may also have contributed to the difficulty of data interpretation.

General Toxicology

Necitumumab was evaluated in 5- and 26-week repeat dose studies in cynomolgus monkeys. There were no significant drug-related findings following dosing for 5 weeks at doses as high as 40 mg/kg. In the 26-week study, monkeys were administered necitumumab weekly by intravenous infusion at doses of 6, 19, or 60 mg/kg. Following 26 weeks of dosing, the skin was found to be the primary target site, similar to the toxicity observed with other EGFR inhibitors. Hyperplastic dermatitis, characterized by epidermal hyperplasia, hyperkeratosis, and inflammatory infiltration was observed grossly and microscopically in skin of the abdomen, inguinal area, ears /nose/mouth, and to a lesser extent, skin of the mammary glands. Findings were observed at all dose levels with a higher incidence at doses ≥ 19 mg/kg. Similarly, skin at the injection site exhibited hyperkeratosis, hyperplasia, hemorrhage, inflammation and lymphocytic infiltration at all doses with a greater incidence at 60 mg/kg. There was a single drug-related death in this study at the high dose level which was believed to be due to septicemia related to skin lesions. In addition, monkeys were treated with antibiotic ointment for skin toxicity on an as needed basis, potentially preventing additional deaths secondary to skin lesions and septicemia. Clinical observations in monkeys were consistent with dose-related skin toxicity and included erythema, scaling, dry skin, and rash. Skin toxicity has previously been observed with similar EGFR inhibitors (e.g. cetuximab), and was the most commonly observed adverse event in patients administered necitumumab (including rash, dermatitis acneiform, acne, pruritus, dry skin, and paronychia).

Magnesium levels were marginally depressed in males and depressed in females at doses ≥ 19 mg/kg. This finding is consistent with hypomagnesemia observed in the clinic. Magnesium levels in monkeys remained depressed following recovery. Degeneration of renal tubular epithelium was observed in monkeys administered necitumumab; specific renal toxicity was not observed clinically, but was consistent with findings observed with cetuximab and may contribute to electrolyte imbalances seen in the clinic. Diffuse inflammation and lymphocytic infiltration was observed in multiple organs and tissues following dosing and recovery in all dose groups. Thromboembolism observed in the clinic was not exhibited in monkeys, though mild increases in platelets occurred at all dose levels compared to controls throughout the 26-week study and extending until the end of the recovery period. Toxicokinetics indicated that necitumumab exposure was generally dose proportional to greater than dose-proportional in monkeys treated for 26 weeks. Meaningful interpretation of immunogenicity data could not be assessed due to the presence of circulating necitumumab.

Reproductive and Development Toxicology

Reproductive toxicity studies using necitumumab were not conducted. Instead the Applicant provided a literature based assessment of the potential for necitumumab to cause developmental toxicity Based on the presented literature, disruption of EGFR can have clear detrimental effects, including significant effects on placental, lung, skin, cardiac, and neural development which can lead to embryofetal and postnatal death, and clear phenotypic signs of teratogenicity. Though the available literature was sufficient to demonstrate a clear requirement for EGFR signaling at multiple points in development, the Applicant also provided surrogate data in a non-human primate study using cetuximab as a surrogate for necitumumab to address whether blocking EGFR signaling with an antibody would result in similar effects to those seen in the knockout animals. The Applicant has the right of reference to the nonclinical reproductive toxicity data for cetuximab (BLA #125,084) and presented pharmacology data showing that cetuximab and necitumumab bind with similar affinities to similar epitopes in domain III of EGFR. The two antibodies also showed comparable in vitro and in vivo pharmacological activity, further supporting the use of cetuximab as a surrogate for necitumumab in the assessment for the potential of necitumumab to cause developmental effects in the context of the available data on EGFR signaling in development.

Human IgG is known to cross the placental barrier. Consistent with this ability, cetuximab was detected in amniotic fluid and the serum of embryos from treated dams. In the developmental toxicity study conducted as a postmarketing requirement for cetuximab, the antibody caused embryolethality and abortions at clinically relevant doses. Necitumumab has the potential to cause fetal harm when administered to pregnant women based on the cetuximab data and the inhibition of EGFR found to be essential for normal organogenesis, proliferation, and differentiation in the developing embryo.

Special Toxicology

Cross reactivity studies were conducted to assess the ability of anti-human EGFR antibody IMC-11F8 (FITC-labeled 11F8) to bind frozen human, monkey and rat tissues. IMC- 11F8 bound to human and monkey EGFR in skin, primarily basal epidermal cells, but not to rat skin. In a separate study, IMC-11F8 reacted with human and monkey epithelium, endocrine cells, myoepithelium, neural tissues, stromal cells, mononuclear/phagocyte cells, smooth muscle and mesothelium. Many tissues displaying IMC-11F8-specific staining were limited to cytoplasmic staining only due to stain limitations

.

12 Appendix/Attachments

None

References

[1] Li S Kussie P, Ferguson KM. 2008. Structural basis for EGF Receptor inhibition by the therapeutic antibody IMC-11F8. Structure. **16(2)**: 216-227.

[2] Li S, Schmitz KR, Jeffrey PD, Wiltzius JJ, Kussie P, Ferguson KM. 2005. Structural basis for inhibition of the epidermal growth factor receptor by cetuximab. Cancer Cell. **7 (4)**, 301-311.

[3] Kamei, Y., Tsutsumi, O., Yamakawa, A., Oka, Y., Taketani, Y., Imaki, J., 1999. Maternal epidermal growth factor deficiency causes fetal hypoglycemia and intrauterine growth retardation in mice: possible involvement of placental glucose transporter GLUT3 expression. Endocrinology. **140**, 4236-4243.

[4] Sibilia, M., Wagner, E.F., 1995. Strain-dependent epithelial defects in mice lacking the EGF receptor. Science. **269**, 234-238.

[5] Miettinen, P.J., Berger, J.E., Meneses, J., Phung, Y., Pedersen, R.A., Werb, Z., Derynck, R., 1995. Epithelial immaturity and multiorgan failure in mice lacking epidermal growth factor receptor. Nature. **376**, 337-341.

[6] Threadgill, D.W., Dlugosz, A.A., Hansen, L.A., Tennenbaum, T., Lichti, U., Yee, D., LaMantia, C., Mourton, T., Herrup, K., Harris, R.C., et al., 1995. Targeted disruption of mouse EGF receptor: effect of genetic background on mutant phenotype. Science. **269**, 230-234.

[7] Sibilia, M., Steinbach, J.P., Stingl, L., Aguzzi, A., Wagner, E.F., 1998. A strain-independent postnatal neurodegeneration in mice lacking the EGF receptor. The EMBO Journal. **17**, 719-731.

[8] Dackor, J., Caron, K.M., Threadgill, D.W., 2009. Placental and embryonic growth restriction in mice with reduced function epidermal growth factor receptor alleles. Genetics **183**, 207-218.

This is a representation of an electronic record that was signed electronically and this page is the manifestation of the electronic signature.

/s/

MARGARET E BROWER
07/23/2015

SHAWNA L WEIS
07/23/2015

WHITNEY S HELMS
07/24/2015

PHARMACOLOGY/TOXICOLOGY FILING CHECKLIST FOR NDA/BLA or Supplement

BLA Number: 125,547 **Applicant: Eli Lily and Co.** **Stamp Date: December 2, 2014**

Drug Name: Necitumumab **BLA Type: Standard review**

On **initial** overview of the BLA application for filing:

	Content Parameter	Yes	No	Comment
1	Is the pharmacology/toxicology section organized in accord with current regulations and guidelines for format and content in a manner to allow substantive review to begin?	X		See additional comment about formatting problem with the long-term general toxicology study (Study (b) (4) .023.07)
2	Is the pharmacology/toxicology section indexed and paginated in a manner allowing substantive review to begin?	X		
3	Is the pharmacology/toxicology section legible so that substantive review can begin?	X		
4	Are all required (*) and requested IND studies (in accord with 505 b1 and b2 including referenced literature) completed and submitted (carcinogenicity, mutagenicity, teratogenicity, effects on fertility, juvenile studies, acute and repeat dose adult animal studies, animal ADME studies, safety pharmacology, etc)?	X		
5	If the formulation to be marketed is different from the formulation used in the toxicology studies, have studies by the appropriate route been conducted with appropriate formulations? (For other than the oral route, some studies may be by routes different from the clinical route intentionally and by desire of the FDA).	NA		
6	Does the route of administration used in the animal studies appear to be the same as the intended human exposure route? If not, has the applicant submitted a rationale to justify the alternative route?	X		
7	Has the applicant submitted a statement(s) that all of the pivotal pharm/tox studies have been performed in accordance with the GLP regulations (21 CFR 58) or an explanation for any significant deviations?	X		
8	Has the applicant submitted all special studies/data requested by the Division during pre-submission discussions?	X		

File name: 5_Pharmacology_Toxicology Filing Checklist for NDA_BLA or Supplement 010908

PHARMACOLOGY/TOXICOLOGY FILING CHECKLIST FOR NDA/BLA or Supplement

	Content Parameter	Yes	No	Comment
9	Are the proposed labeling sections relative to pharmacology/toxicology appropriate (including human dose multiples expressed in either mg/m2 or comparative serum/plasma levels) and in accordance with 201.57?	X		
10	Have any impurity – etc. issues been addressed? (New toxicity studies may not be needed.)			Additional review needed
11	Has the applicant addressed any abuse potential issues in the submission?	NA		
12	If this NDA/BLA is to support a Rx to OTC switch, have all relevant studies been submitted?	NA		

IS THE PHARMACOLOGY/TOXICOLOGY SECTION OF THE APPLICATION FILEABLE? ___Yes_____

If the NDA/BLA is not fileable from the pharmacology/toxicology perspective, state the reasons and provide comments to be sent to the Applicant.

Please identify and list any potential review issues to be forwarded to the Applicant for the 74-day letter.

The formatting and spacing in Study (b) (4) 023.07 needs to be corrected. There are odd spaces in the text and tables and a problem making the tables unreadable. Submit a corrected version of this report by January 30th. In the resubmission describe any other changes made to the final report.

Reviewing Pharmacologist Date

Team Leader/Supervisor Date

File name: 5_Pharmacology_Toxicology Filing Checklist for NDA_BLA or Supplement 010908

This is a representation of an electronic record that was signed electronically and this page is the manifestation of the electronic signature.

/s/

MARGARET E BROWER
01/23/2015

WHITNEY S HELMS
01/27/2015